DETERMINATION OF INTERNAL CONVERSION COEFFICIENTS BY THE SCINTILLATION METHOD

By

BUFORD RAY ANDERSON

Bachelor of Science

Murray State College

Murray, Kentucky

1960

Submitted to the faculty of the Graduate School of
the Oklahoma State University
in partial fulfillment of the requirements
for the degree of
MASTER OF SCIENCE
May, 1963

DETERMINATION OF INTERNAL CONVERSION COEFFICIENTS

BY THE SCINTILLATION METHOD

Thesis Approved:

Henry Palmer Klotz
Thesis Adviser

H. H. Harrington

Lowell MacVicar
Dean of the Graduate School

PREFACE

For the determination of internal conversion coefficients β-spectrometer methods have been used most commonly. These methods, however, fail just in the interesting case of isomers not following an intense branch in β-decay or K-capture, or in cases where the conversion coefficient is high. In these cases comparison of the gamma and x ray intensities is almost inevitable and is usually accomplished by use of a scintillation spectrometer. In cases where the conversion coefficients can be found by both β-spectrometer and scintillation methods, the results have found to be in good agreement.

The author is indebted to Dr. H. P. Hotz for his valuable guidance, continuous aid and encouragement during the execution of this work. I would also like to express my appreciation to Professor C. F. Harris for the loan of the sources; to Mr. C. Northup for helpful discussions; and to Dr. B. C. Groseclose and Mr. G. D. Loper for assistance and loan of equipment.

TABLE OF CONTENTS

LIST OF TABLES

LIST OF FIGURES

INTRODUCTION

Definition of Internal Conversion

Internal Conversion is usually referred to in the following way. When a nucleus is in an excited state for which the excitation energy is less than the binding energy of a nuclear particle, the nucleus will go to a lower energy state predominantly by either one of two competing processes. Either a gamma ray photon will be emitted or the nuclear excitation energy will be transferred to one of the orbital electrons by interaction of one of the nucleons with an orbital electron resulting the ejection of the orbital electron from the atom, the latter process is referred to as internal conversion (1). With the transition energy greater than 1.02 MeV, there is a possibility of an electron-positron pair being emitted instead of an orbital electron or photon and this takes place but with a frequency very small relative to gamma emission. If we let the decay constant λ_q represent the probability per second for the emission of a photon, whose energy is $hf = kmc^2$, by a radiative nuclear multipole transition, and the decay λ_e represent the probability per second that this same nuclear multipole field will transfer its energy $hf = kmc^2$ to any bound electron in its own atom, then the total internal conversion coefficient α is defined as (2) $\alpha \equiv \lambda_e/\lambda_q = N_e/N_q$. The ratio N_e/N_q is sometimes called the branching ratio where, N_e is the number of conversion electrons per second and N_q is the number of photons per second. The total transition probability is then,

$\lambda_t = \lambda_q + \lambda_e$ and the total number of nuclei transforming is $N_q + N_e$ or $N_q(1 + \alpha)$.

Discussion of Internal Conversion Coefficients

It will be shown in the theory section that the internal conversion coefficients will depend on many things of interest such as the energy of transition, the atomic number of the emitter, the shell or subshell from which the electron is ejected, the multipolarity L of the angular momentum of the radiated field, and the character of the transition, electric or magnetic. Usually when the nuclear excitation energy is small and the angular momentum change is large, internal conversion will predominate over gamma emission. In this case the nuclear excitation energy is transferred to one of the penetrating orbital electrons, usually a K electron, resulting in the electron being ejected from the atom. This produces vacancies in the K shell and other shells of the atomic electrons but with the majority of the vacancies in the K shell. Therefore internal conversion transitions are accompanied by x ray emission spectra. No change in nuclear charge is involved with internal conversion or gamma emission so the x ray spectra are characteristic of the element in which the nuclear transition took place. The relative probability that a vacancy in the K shell is filled under emission of K x ray is called the "Fluorescent Yield" of the K shell, ω_k. According to Burhop (3) ω_k depends on the nuclear charge as:

$$(\omega_k / 1-\omega_k)^{\frac{1}{4}} = -A + BZ - CZ^3$$

Values for the constants A, B, and C have been given by Burhop and by Roos (4). More recent data has been used by Hagedoorn and Wapstra (5) to derive these constants and they tend to give somewhat lower values

in the region $20<Z<30$ than those of Burhop or Roos.

The vacancies in the atomic shells due to internal conversion are filled again by electrons from outer shells and the energy released may be carried off by an x ray quantum or it can be transferred to another electron which is then ejected from the atom. Such an electron is called an "Auger Electron" (6). The resulting atom is ionized in two shells, which may be identical. In almost the same way as fluorescence yield one can define an auger yield and these can be used in determining internal conversion coefficients.

During the past three decades many measurements of internal conversion coefficients have been made and the theory of internal conversion of gamma rays has been improved by several people (7, 8, 9, 10, 11). Calculations of the theoretical values of internal conversion coefficients (12, 13, 14, 15, 16) have been made and those for the K shell are thought to be good to within less than one per cent. Most of the measurements have been in agreement with the theory and have served as a significant test for the theory although their accuracy in some instances was not within one per cent. The first people to measure the internal conversion coefficients for the two gamma rays in the decay of Co^{60} were Deutsch and Siegbahn (17) at the Nobel Institute for Physics. They used a large double-focusing spectrometer which permitted a resolution of one per cent. Comparison of their results with the theoretical values of Rose (16) indicated that the parity change must be the same in both transitions and that the two gamma rays are probably electric quadrupoles. Waggoner, Moon, and Roberts (18) used a double coil, thin lens magnetic beta-ray spectrometer to measure the internal conversion coefficients of the gamma rays from Co^{60}, Cs^{134}, and Zn^{65}. The

results obtained compare well with the theoretical values and indicate that both of the gamma rays from Co^{60} are electric quadrupoles. Also using a double lens beta ray spectrometer but with a thin window, the internal conversion coefficients of Co^{60} were investigated by Fan (19). The results of all the previous measurements of Co^{60} can be put in the following table.

TABLE I

PREVIOUS RESULTS FRO Co^{60}
α (10^4)

	Exp.		Theor.	
	Gamma		EQ	MD
Deutsch and Siegbahn	1.17 MeV	2.32 ± 0.6	1.545	1.387
	1.33 MeV	1.83 ± 0.5	1.175	1.034
Waggoner, Moon, and Roberts	1.17 MeV	1.733 ± 0.061		
	1.33 MeV	1.286 ± 0.035		
Fan, Chang-Yun	1.17 MeV	1.72 ± 0.17		
	1.33 MeV	1.24 ± 0.12		

Since all the previous measurements shown in Table I were made with high resolution beta ray spectrometers, they are expected to be more accurate than the measurements in the present study, but our scintillation spectrometer measurements agree well with the previous measurements. The scintillation spectrometer does not have the high resolution of the beta ray spectrometer but has the advantage of measuring weak sources. In most cases where internal conversion coefficients are to be measured both types of spectrometers are usually employed.

The Scintillation Spectrometer

A phosphor coupled to a photomultiplier tube was first successfully used to detect ionizing radiation in about 1944. Since that time

phosphors have been used in a variety of ways for detecting different types of ionizing radiation. Some of the characteristics of this type of detector compared to other means of measurement are high sensitivity to gamma rays, response proportional to the incident radiation, rapid response time and fast decay times. Sodium iodide, activated with thallium, combines a number of excellent properties which make it one of the most important scintillation phosphors. NaI(Tl) has about the highest energy conversion efficiency of any known phosphor and can be grown in large single transparent crystals. So as a scintillator for spectrometric measurements, NaI(Tl) is probably superior to any other material so far known.

The working principle of a scintillation spectrometer can be summarized in the following way. A gamma or x ray quantum being absorbed in the NaI(Tl) crystal causes a light flash. This light flash on the photosensitive cathode of the photomultiplier causes an avalanche of electrons to reach the anode of the photomultiplier tube. This generates a pulse which is amplified many times by a non-overloading linear amplifier. With many pulses being amplified they can be sorted by use of a single channel pulse height analyzer and counted separately by a scaler. A block diagram of the instrument is given in Figure 1, and a full discussion of the various components will be given in Chapter III.

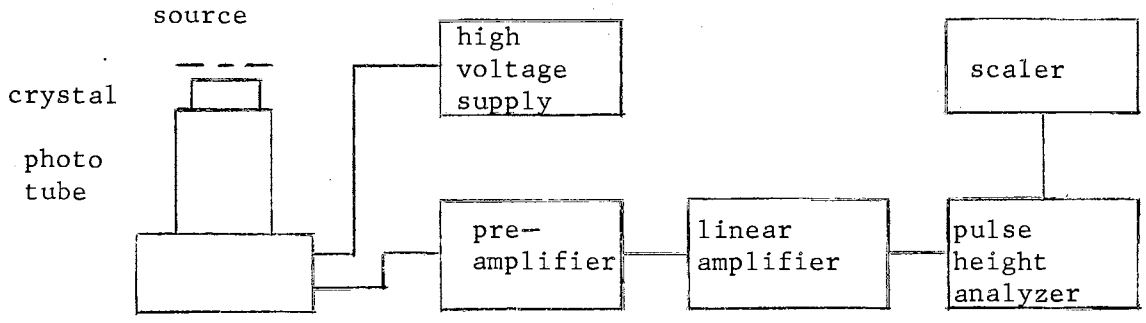

Figure 1. Block Diagram of a Scintillation Spectrometer

All processes involved are linear and a curve showing the number of pulses of a certain amplitude versus the amplitude (pulse height) gives information about the energy spectrum of the absorbed radiation. A typical scintillation spectrum of a single gamma ray is shown in Figure 2 and may contain the following features: a photopeak at a pulse height corresponding with the gamma ray energy E, pair peaks at E-1022 keV and at E-511 keV, and escape peak (Figure 3) at E = E -28.5 keV, and a Compton continuum containing all energies up to $E - E'_{\pi}$. The energy of gamma rays with initial energy E becomes after Compton scattering through an angle θ,

$$E'_{\theta} = \frac{m_o c^2}{\{(m_o c^2/E) + 2\}}$$

and the minimum remaining energy is obtained in back scattering ($\theta = \pi$)

$$E'_{\pi} = \frac{m_o c^2}{\{(m_o c^2/E) + 2\}}$$

A backscattering peak at energies slightly higher than E'_{π} is an always present spurious feature and its intensity depends on the counting arrangement.

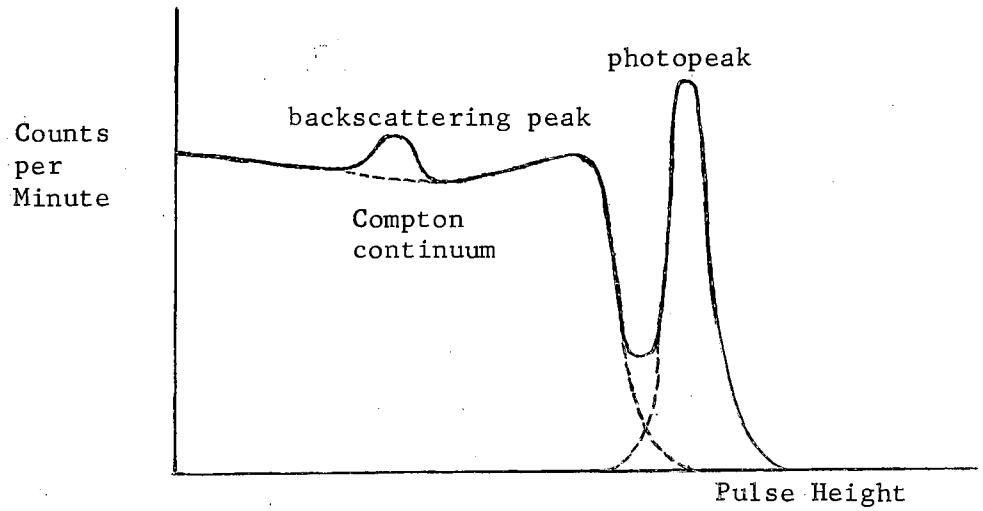

Figure 2. Scintillation Spectrum of a ~ 1 MeV Gamma Ray

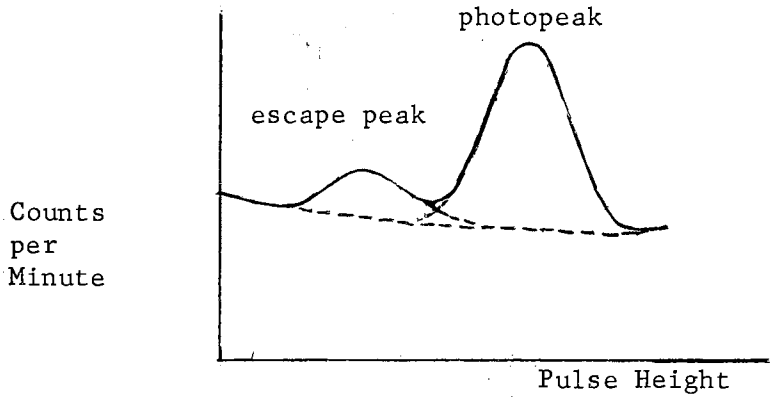

Figure 3 Scintillation Spectrum of an ~ 60 keV Gamma Ray

Some of the problems involved with the scintillation spectrometer can now be pointed out, however they will be discussed further in Chapter III. The efficiency of the scintillation spectrometer is a function of the gamma ray energy so the spectrometer has to be calibrated at various energies. At low energy this efficiency can be computed but at higher energies the computation is complicated due to the second order processes (20). At low energies the Compton absorption cross-section is negligible compared to the photo absorption cross-section and in this case for energies lower than 100 keV.

The complex gamma ray spectra can be analyzed into components by successively subtracting the single spectra due to the highest energy gamma ray (21). For low energy lines, which are broad and accompanied by escape peaks, the separation from the background due to Compton continuum of higher energy gamma rays is not easily accomplished. However, a knowledge of the ratio of the area under the escape peak and that under the photo peak will help in separating such peaks from the background.

The commercially canned crystal is covered with an Al_2O_3 reflector

and Al container. Necessary corrections for absorption must be made especially for the x rays.

THEORY

Theory of Inorganic Crystal Scintillators

In the present study we are more specifically interested in the photoelectric process produced by x and γ radiation in an inorganic solid and by visible and ultraviolet photons at metal surfaces. A discussion of the effect at metal surfaces can be found in most text books and can be extended to include interaction of quanta with electrons bound to individual atoms. In an inorganic crystal such as sodium iodide activated with thallium, the mechanism for the production of the scintillation can be described best in terms of the band picture of solids (22, 23). Sodium iodide activated with thallium belongs to the class of ionic crystals as classified by Seitz (24). The electronic energy states of a single atom or molecule are a series of discrete levels, however in an inorganic crystal lattice the outer electron energy levels are perturbed by mutual interactions between the atoms or ions. These levels are broadened into a series of continuous "allowed" energy bands, separated by "forbidden" regions of energy. The inner electronic levels of the atom are practically undisturbed and retain their normal character. For an insulator the energy band system is shown in Figure 4 such that in the normal state, the lower energy bands are completely filled, while the higher bands are empty. The bands extend through the crystal, and electrons are free to move in them without additional activation energy. Motion through a filled

band does not cause electrical conduction, since equal numbers of electrons move in opposite directions. The highest filled band is separated from the lowest empty band by an energy of a few electron volts. Electrons in the filled band may be raised into the empty bands by the absorption of quanta, having positive holes in the filled band. Photoconductivity then occurs due to the motion of the excited electrons and positive holes.

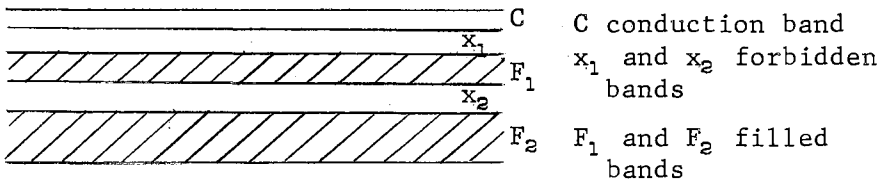

Figure 4. Energy Band System of an Insulator

This simple model applies only to insulators having a perfect crystal lattice. In practice, variation due to lattice defects, etc., occur in the energy bands producing local electronic energy levels in the normally forbidden region below the conduction band. If these levels are unoccupied, electrons moving in the conduction band in their vicinity may drop to the valence band by emission of photons and this is the process of fluorescence. Most inorganic crystalline phosphors are activated by the inclusion of impurity atoms in the crystal lattice. Additional energy levels are introduced locally by the impurity ions which creates fluorescent centers (25). The energy band for an impurity-activated phosphor is shown in Figure 5.

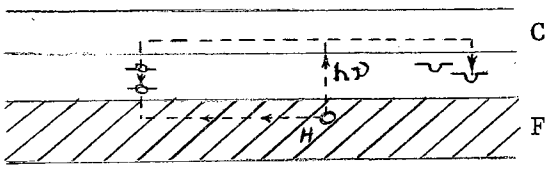

Figure 5. Energy Band for an Impurity-Activated Phosphor

An excited electron in the conduction band may lose its energy without the emission of photons, say to thermal energy or lattice vibration. This process is referred to as one of quenching and it might be pointed out that the temperature effects are very important. Another possibility is the trapping of the electron at the energy associated with the impurity atoms. When this occurs, the level is referred to as a metastable state. The electron will remain in the metastable state until raised again to the conduction band or until it drops to the valence band with the emission of a quantum. From the conduction band the electron can undergo any of the three processes just described. If, after being trapped in the metastable state, the electron drops to the valence band with the emission of photons, the phenomenon is phosphorescence.

Theory of Internal Conversion

A nucleus in an excited state, for which the excitation energy is less than the binding energy of a nuclear particle, may emit a gamma ray in making a transition to a state of lower energy or the energy released may be utilized to eject an atomic electron from one of the bound states into the continuous energy spectrum. These two processes are competing in the sense that one or the other takes place when a given nucleus makes a transition provided the energy is less than 1.02 MeV. If the energy is greater than 1.02 MeV then there is a possibility of the energy appearing as an electron-positron pair. The internal conversion coefficient is a measure of the relative probability of the processes and is defined as the ratio of the total number of ejected (conversion) electrons per unit time to the total rate of emission of gamma rays. The theoretical treatment which follows is essentially that of Preston (54).

In order to obtain an internal conversion coefficient we will consider the interaction between two particales which takes place by the way of the coupling of each particle with the radiation field. We must consider the quantum-mechanical description of the interaction energy. One of these particles will be taken to be a Dirac electron and the other to be a nucleon to which the radiation field is coupled. The equations of motion for a nucleus coupled to an electromagnetic field depend intimately on the essentially unknown nuclear forces, but for the internal conversion coefficient of a point nucleus it is unnecessary to specify the nuclear dynamics in detail.

We will consider a total system that consists of the radiation field and two particles with subscripts 1 and 2. We will let particle 1 be a Dirac electron and particle 2 a nucleon to which the radiation field is coupled. The hamiltonian equation for the system is

$$i \frac{\partial \psi}{\partial t} = [H_1(\bar{A}) + H_2(\bar{A}) + H_r)]\psi \tag{2.1}$$

where t designates the time and the units are such that, in this equation, H_r is the hamiltonian of the radiation field alone; $H_1(\bar{A})$ and $H_2(\bar{A})$ refer to particles 1 and 2 in the presence of the field, whose vector potential is $\bar{A}$. Thus H_1 and H_2 contain the coupling terms which represent the interaction between particles and field.

For the Dirac electron

$$H_1 = -\alpha \cdot (\vec{p} - e_1 \bar{A}) - \beta m + e_1 \bar{U} \tag{2.2}$$

where e_1 is the electron charge, m the electron mass, the matrices α and β are

$$\alpha = \begin{pmatrix} 0 & \sigma \\ \sigma & 0 \end{pmatrix} \qquad \beta = \begin{pmatrix} 1 & 0 \\ 0 & -1 \end{pmatrix}$$

where each element is a two-by-two matrix and σ is defined as

$$\vec{\sigma} = \frac{\hbar}{2} \vec{s}.$$

H_1 can also be written as

$$H_1 = H_1(0) + H_1(\bar{A}) \tag{2.3}$$

where

$$H_1(0) = -\alpha \cdot p - \beta m \tag{2.4}$$

is the free particle hamiltonian and

$$H_1(\bar{A}) = e_1(\alpha \cdot \bar{A} + \bar{U}) \tag{2.5}$$

is the coupling term. Corresponding to the decomposition of $\bar{A}$ and $\bar{U}$ into complex fields, we have

$$H_1(\bar{A}) = H_1(A)e^{-i\omega t} + H_1(A^*)e^{i\omega t} \tag{2.6}$$

and $H_1(A)$ is the functional of A defined by the form of Equation 2.3.

It is essential to consider the effect of a gauge transformation. If the wave functional ψ describes the Dirac electron so that

$$i\frac{\partial \psi}{\partial t} = H_1 \psi \tag{2.7}$$

and we make the transformation

$$\psi = e^{-ie_1\bar{S}}\psi' \tag{2.8}$$

where $\bar{S}$ is a (one-by-one) function of the coordinates and time, it follows that

$$i\frac{\partial \psi'}{\partial t} = H_1'\psi' \tag{2.9}$$

where

$$H_1' = e^{ie_1\bar{S}} H_1 e^{-ie_1\bar{S}} - e_1\frac{\partial \bar{S}}{\partial t} \tag{2.10}$$

where H_1 is given by (2.2). This result (2.10) is quite general and describes the effect of the unitary transformation on ($\bar{S}$ hermitian) any hamiltonian equation. It follows that

$$H_1'(\bar{A}) = H_1(\bar{A}') \tag{2.11}$$

where $\bar{A}'$ stands for the gauge-transformed potentials. Equation 2.11

then states that a gauge transformation on the potential is equivalent to a canonical transformation (unitary) on the basis ψ. A canonical transformation does not change the matrix elements of the coupling operators, and we can conclude that the transition probabilities are independent of the gauge as long as the property expressed by Equation 2.11 is fulfilled. That is, the hamiltonian for which Equation 2.11 is fulfilled is then said to be gauge invariant.

For the Dirac electron the construction of the gauge-invariant hamilton is given by Equation 2.2. However, if there are interaction terms, such as those representing the nuclear forces in $H_2(0)$, which do not commute with $\bar{S}$, the gauge-invariant hamiltonian may be much more complicated and its exact form depends on the nature of these nuclear interactions. Since these nuclear interactions are not completely understood, the interaction will be treated in a general way. So for particle 2 we write,

$$H_2(\bar{A}) = H(0) + H^{(1)}(\bar{A}) + H^{(2)}(\bar{A}) + \ldots \qquad (2.12)$$

which corresponds to an expansion in the vector potential or coupling constant e_2. Thus $H(0)$ is the free-particle hamiltonian, $H^{(1)}(\bar{A})$ is homogeneous and of second degree in $\bar{A}$, etc. Each term in Equation 2.12 is hermitian. Since we are interested only in single quantum emission or absorption, the terms beyond $H^{(1)}$ will be dropped. So we write,

$$H^{(1)}(\bar{A}) = H^{(1)}(A)e^{-i\omega t} + H^{(1)}(A^*)e^{i\omega t} \qquad (2.13)$$

where A, A* are time independent.

Consider the following situation: At t = 0, particle 1 is in a state of zero energy, particle 2 in an excited state of energy W. This is the initial state and will be given the subscript i. There are two intermediate states described by the following scheme:

	Particle 1	Particle 2	quantum energy
State j	0	0	ω
State j'	E	W	ω

That is, for state j a (virtual) quantum of energy ω has been emitted by particle 2 whose energy after emission is zero. For state j' a quantum of energy ω has been emitted by particle 1 which takes the energy E after emission. The final state, with subscript f, is one in which there are no radiation quanta, particle 1 is in the state with energy E, and particle 2 is in the state with zero energy. This state is reached from j or j' by absorption of radiation energy ω by particle 1 or 2.

The total wave function Ψ is expanded into functionals of states, i, j, j', f:

$$\Psi = a_i(t)\Psi_i + a_j(t)\Psi_j + a_{j'}(t)\Psi_{j'} + a_f(t)\Psi_f \tag{2.15}$$

Then the equations of motion for the probability amplitudes a_i ------ a_f take the form (26)

$$i\dot{a}_i = wa_i + \int d\omega H_{o\omega} a_j(\omega) + \int d\omega H'_{o\omega} a_{j'}(\omega) \tag{2.16a}$$

$$i\dot{a}_j = \omega a_j + H_{o\omega} a_i + \int dE H_{\omega E} a_f(E) \tag{2.16b}$$

$$i\dot{a}_{j'} = (\omega + w + E)a_{j'} + H'_{\omega o} a_i + \int dE H'_{\omega E} a_f(E) \tag{2.16c}$$

$$i\dot{a}_f = Ea_f + \int d\omega H_{E\omega} a_j(\omega) + \int d\omega H'_{E\omega} a_{j'}(\omega) \tag{2.16d}$$

Here $\int d\omega$ implies an integration over all intermediate photon energies and a sum over e, 1, M, that is, over the complete set of multipole fields (27) in terms of which the general radiation field is expanded, as in Appendix A. The integration designated by $\int dE$ sums over the energies of the Dirac electron and also implies a spin summation. The matrix elements are defined by

$$H_{\varepsilon\omega} = e(2\pi/\omega)^{\frac{1}{2}}\int d\tau\psi_f^*[\alpha\cdot A_{LM}^{(i)}(\omega r) + i\varphi_L^{M(i)}(\omega r)]\psi_i \quad (2.17a)$$

$$H'_{\varepsilon\omega} = e'(2\pi/\omega)^{\frac{1}{2}}\int\alpha'\cdot A_{LM}^{(i)}(\omega r') + i\varphi_L^{M(i)}(\omega r')]\Phi_i \quad (2.16b)$$

$$H_{\omega o} = e'(2\pi/\omega)^{\frac{1}{2}}\int\alpha'\cdot A_{LM}^{(i)}(\omega r') - i\Phi_L^{M(i)*}(\omega r')]\Phi_i \quad (2.17c)$$

$$H'_{\omega o} = e\ (2\pi/\omega)^{\frac{1}{2}}\int d\tau\psi_f{}^*[\alpha\cdot A_{LM}^{(i)*}(\omega r) - i\varphi_L^{M(i)*}(\omega r)]\psi_i \quad (2.17d)$$

in which ψ and Φ are, respectively, the electronic and nuclear wave functions with the subscripts i and f referring to the initial and final states. Here e, r, $d\tau$ and α refer, respectively, to the charge, position, volume element, and Dirac operator for the electron. The corresponding primed quantities refer to the nucleus and $A_{LM}^{(i)}$ and $\varphi_L^{M(i)}$ are, respectively, the vector and scalar potentials for the 2^L-th multipole of the i-th type (electric, magnetic, or longitudinal).

The equations for the probability amplitudes can be solved by the use of Laplace transformation (28). No assumption as to the general form of the solution has to be made so denoting the laplace transforms by the use of capitals, we have

$$L\{a_i\} = A_i = \int_o^\infty e^{-St}a_i(t)dt$$

where $S = \eta - ik$, and $\eta \geq 0$. After applying the initial conditions $a_i = 1 \quad a_j = a_{j'} = a_f = 0$ and making the substitution $\omega_o = w + E - k$, the transforms of equations 2.16 are

$$(w - k - i\eta)A_i = -i - \int d\omega H_{o\omega}A_j - \int d\omega H'_{o\omega}A_{j'} \quad (2.18a)$$

$$(\omega - k - i\eta)A_j = - H_{\omega o}A_i - \int dE H_{\omega\varepsilon}A_f \quad (2.18b)$$

$$(\omega + \omega_o - i\eta)A_j = - H'_{\omega o}A_i - \int dE H'_{\omega\varepsilon}A_f \quad (2.18c)$$

$$(E - k - i\eta)A_f = - \int d\omega H_{\varepsilon\omega}A_j - \int d\omega H'_{\varepsilon\omega}A_{j'} \quad (2.18d)$$

For the radiation processes which we are considering, $|a_f|^2$ is proportional to e^4. Therefore, as will be seen from the math below, A_i must be determined in fourth approximation. The zeroth approximation of A_i gives a(t) as a periodic function of the time; the second

approximation gives the decay of a(t) with the emission of the gamma-quantum; and the fourth approximation gives the decay of a(t) with both the emission of the gamma-quantum and the ejection of the orbital electron. Since the first approximation does not include the effect of the presence of the other electrons, A_j need be determined in third approximation; A_f need be determined in second approximation only.

In zeroth approximation (2.18a) gives

$$(w - k - i\eta)A_i = -i. \tag{2.19}$$

Substitution of (2.19) into (2.18b, c) yields A_j and $A_{j'}$ in first approximation.

$$(\omega - k - i\eta)A_j = -H_{\omega o}A_i \tag{2.20}$$

$$(\omega + \omega o - i\eta)A_{j'} = -H'_{\omega o}A_i \tag{2.21}$$

Substitution of (2.20, 21) into 2.18d) gives A_f in second approximation.

$$(E - k - i\eta)A_f - A_i\int d\omega\left[\frac{H_{\varepsilon\omega}H_{\omega o}}{\omega - k - i\eta} + \frac{H'_{\varepsilon\omega}H'_{\omega o}}{\omega + \omega_o - i\eta}\right] \tag{2.22}$$

where the integral over ω, which we denote by U_{fo} is evaluated in Appendix B.

$$U_{fo} = -ee'\int d\tau\int d\tau'\,\psi_f^*\Phi_f^*\,(1 - \alpha\cdot\alpha')\left(\frac{e^{ikX}}{X}\right)\psi_i\,\Phi_i$$

Substitution of (2.20, 21) into (2.18a) gives A_i in second approximation.

$$(w - k - i\eta)A_i = -i - A_i\int d\omega\left[\frac{H_{o\omega}H_{\omega o}}{\omega - k - i\eta} + \frac{H'_{o\omega}H'_{\omega o}}{\omega + \omega_o - i\eta}\right] \tag{2.23}$$

where the integral over ω, which we denote by $i\gamma_1$, γ_1 being real and positive, is evaluated in Appendix B. Substitution of (2.22, 23) into (2.18b, c) gives A_j and $A_{j'}$ in the third approximation:

$$(\omega - k - i\eta)A_j = -H_{\omega o}A_i - U_{fo}A_i\int dE\left\{\frac{H_{\omega E}}{E - k - i\eta}\right\} \tag{2.24}$$

and

$$= -A_i\left[H_{\omega o} + i\pi U_{fo}H'_{\omega k}\right]$$

$$(\omega + \omega_o - i\eta)A_{j'} = -A_i\left[H'_{\omega o} + i\pi U_{fo}H'_{\omega k}\right] \tag{2.25}$$

where $H_{\omega k}$ is $H_{\omega E}$ with E replaced by k and likewise for $H'_{\omega k}$. The evaluation of the integrals over E is discussed in Appendix B.

Substituting (2.24, 25) into (2.18a) gives A_i to the fourth approximation:

$$(w - k - i\eta)A_i = -i + \gamma_1 A_i + i\pi U_{fo} A_i \int d\omega \left[\frac{H_{o\omega} H_{\omega k}}{\omega - k - i\eta} + \frac{H'_{o\omega} H'_{\omega k}}{\omega - \omega_o - i\eta}\right]$$

where the integral over ω, which will be denoted by $U_{of} - U^*_{fo}$ is evaluated in Appendix B. Then writing $\gamma_2 = \pi |U_{fo}|^2$

$$A_i = \frac{-i}{[w-k-i(\eta+\gamma_1+\gamma_2)]} \tag{2.26}$$

Substitution of (2.26) into (2.22, 24) gives

$$A_f = \frac{-iU_{fo}}{(E-k-i\eta)[w-k-i(\eta+\gamma_1+\gamma_2)]} \tag{2.27}$$

$$A_j = \frac{-i[H_{\omega o} + i\pi U_{fo} H_{\omega k}]}{(\omega-k-i\eta)[w-k-i(\eta+\gamma_1+\gamma_2)]} \tag{2.28}$$

The inverse transforms of (2.26, 27, 28) can be obtained and they are

$$a_i(t) = e^{[-iwt-(\gamma_1+\gamma_2)t]} \tag{2.29}$$

$$a_j(t) = \frac{[H_{\omega o} + i\pi U_{fo} H_{\omega k}]\{e^{-i\omega t} - a_i(t)\}}{\omega - w + i(\gamma_1+\gamma_2)} \tag{2.30}$$

$$a_f(t) = \frac{-U_{fo}\{e^{-iEt} - a_i(t)\}}{E-w+i(\gamma_1+\gamma_2)} \tag{2.31}$$

Hence,

$$N_e = \int dE\, |a_f(\infty)|^2 = \frac{\pi}{\gamma_1+\gamma_2} |U_{fo}|^2 \tag{2.32}$$

and

$$N_q = \int d\omega\, |a_j(\infty)|^2 = \frac{\pi}{\gamma_1+\gamma_2} |H'_{\omega o} + i\pi U_{fo} H_{\omega k}|^2 \tag{2.33}$$

Thus, it is seen that N_q is proportional to $|H_{\omega o} + i\pi U_{fo} H_{\omega k}|^2$ rather than $|H_{\omega o}|^2$.

The second term in (2.33) represents the effect of the presence of the extra-nuclear electrons. In the case in which the radiation field is restricted to a given multipole,

$$H_{\omega_o} + i\pi U_{f\circ} H_{\omega k} = e'(2\pi/k)^{\frac{1}{2}} \int d\tau' \Phi_f^* [\alpha \cdot A_{LM}^*(kr') - i\varphi_L^{M*}(kr')] \Phi_i$$
$$X\Big(1 - (2\pi^3 e^2/k) x \{\int d\tau \psi_f^* [\alpha \cdot B_{LM}(kr) + i\psi_L^M(kr)] \psi_i\}$$
$$X\{\int d\tau \psi_f^* [\alpha \cdot A_{LM}^*(kr) - i\varphi_L^{M*}(kr)] \psi_f\}\Big). \quad (2.34)$$

This result agrees with the correspondence principle result of Taylor and Mott (29) and shows that the number of quanta leaving the atom differs from the number ejected from the bare nucleus by a factor of order e^2. The first bracket in the correction term represents the matrix element for electron transitions from bound to continuum state, that is, the matrix element for the absorption of a gamma-quantum, while the second bracket represents the matrix element for the emission of a gamma-quantum. The correction term therefore represents an interference between the two radiation fields involved.

Neglecting the factor of order e^2, the internal conversion coefficient for the given multipole radiation is

$$\alpha(i,L) = (2\pi^3 e^2/k) \left| \int d\tau \psi_f^* [\alpha \cdot B_{LM}(kr) + i\psi_L^M(kr)] \psi_i \right|^2 . \quad (2.35)$$

If we make the assumption of a point nucleus, the matrix element in nuclear space will cancel out and the internal conversion coefficient is then independent of any unknown nuclear properties. The only role which the nucleus plays is to act as a source of a "virtual" electromagnetic field with specified energy, angular momentum, and parity. The fact that the latter two properties condition the conversion coefficient constitutes the reason for the importance of this quantity in nuclear physics. In fact, the conversion coefficient is, in general, a rather sensitive function of k, L, and the character of the transition

(electric or magnetic).

The effect of the finite size of the nucleus on the internal conversion coefficient is incorporated in the previous results, however, there is a question as to the gauge to be used in the investigation. There is a contribution from inside the nucleus to the internal conversion coefficient, but the range of r for the calculation of internal conversion coefficients is taken as $0<r<\infty$. The question arises as to whether or not an extension of the range of r may be carried out with the radiation potentials expressed in terms of any arbitrary gauge. The answer is in the negative as pointed out by Dancoff and Morrison (30).

If, by a gauge transformation, we obtain another set of potentials for which the integrand of the matrix element is small at the origin, this latter set can be called correct. This condition is satisfied by the conventional gauge.

The effect of the finite nuclear size on internal conversion has been studied by Church and Weneser (31) especially for magnetic dipole transitions. Internal conversion coefficients have been found in some cases to disagree with the calculated values by almost an order of magnitude. A theory of these anomalous terms in electric Dipole transitions has been worked out by Nilsson and Rasmussen (32) and several of these cases have been investigated experimentally. This means that internal conversion is not the clear cut tool in nuclear physics that it was once thought to be, but there is an advantage to the effect of the finite nuclear size in that more information should be made available by a study of these internal conversion coefficients. In cases where the coefficients are high, they will be easier to measure by scintillation

spectroscopy experiments.

APPARATUS AND EXPERIMENTAL METHOD

Apparatus

The apparatus consists of the following components: source holder, NaI(Tl) crystal, DuMont 6292 photomultiplier tube and bleeder circuit, Hamner high voltage power supply, Sola constant voltage transformer, preamplifier, linear non-overloading amplifier, single-channel pulse height analyzer, and scalar. The source holder was made of two aluminum rings and mylar foil. The source was sandwiched between two pieces of mylar and held in position by clamping the mylar between the two aluminum rings. The smaller ring has an inside diameter of 2.5 inches and an outside diameter of 2.75 inches. The large ring has inside diameters 2.5 and 2.75 inches and an outside diameter of 3 inches.

The sodium iodide crystal activated with thallium (Harshaw type 8D8) was 2 inches in diameter and 2 inches thick. The crystal was contained in an aluminum can with a 0.125 inch glass optical window. A reflector made of Al_2O_3 was used between the crystal and the housing. The wavelength for maximum emission is about 4100 A and the crystal has a density of 3.67 grams per cubic centimeter which is desirable for the absorption of the gamma rays and the short decay time was also desirable for fast counting.

The NaI(Tl) crystal was mounted on the photomultiplier tube using Dow Corning (Type QC-2-0057) silicone grease as an optical joint.

Considerable care was taken to clean these two areas and a thin film of the silicone grease was spread over the two areas. The crystal was then moved from the side onto the top of the photomultiplier tube so that no air bubbles would be trapped between the two surfaces. The photomultiplier tube and crystal were then wrapped with black electrical tape which served as a light shield.

The photomultiplier tube used was a DuMont 6292. This tube has ten stages and a flat end-window type photocathode having a S-11 spectral response. The tube is 2 inches in diameter and has a focusing shield that can be adjusted to have optimum collection of photoelectrons which is accomplished by varying the potential between the shield and the photocathode as shown in Figure 6.

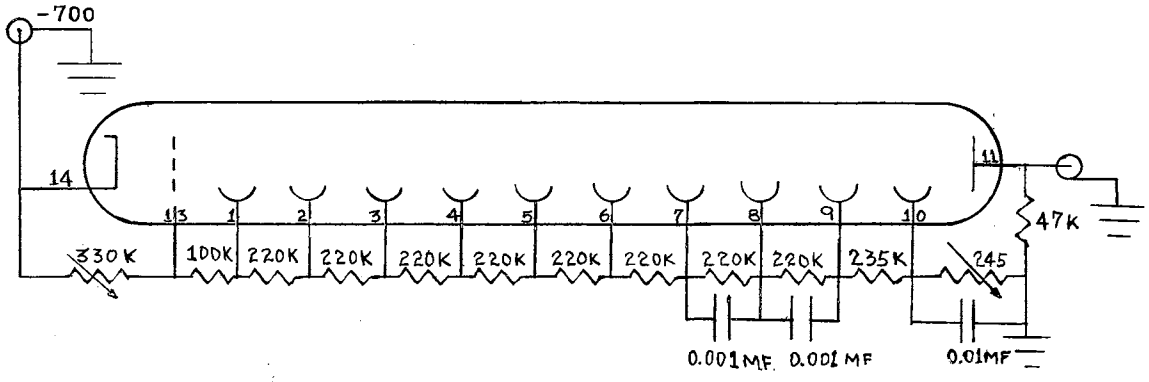

Figure 6. Bleeder circuit for 6292 Photomultiplier Tube

The 6292 tube has stability over long periods of time due to the materials, construction, and arrangement of the dynodes within the tube. Potentials as high as 190 volts per stage may be used for maximum amplification and sensitivity, but for optimum performance and best comprimise between signal-to-noise ratio and amplification, potentials less than 125 volts per stage were used.

The bleeder circuit was housed in an aluminum chassis box separate

from the preamplifier. The resistors had tolerances of ± one per cent with the resistance between the plate and last dynode being variable. This resistance can be adjusted to correct any secondary emission effects that might occur. Negative high voltage was applied and the output is a negative pulse which is developed at the plate (pin 11).

The preamplifier used was a Baird-Atomic Model 231 which uses a stacked follower circuit. The preamplifier serves as an impedance matching device between the photomultiplier and the non-overloading amplifier and has a gain of almost one. The output of the preamplifier is then coupled to a Baird-Atomic Model 215 linear non-overloading amplifier. The Model 215 is a linear pulse amplifier and capable of fast recovery after severe overload. It can amplify small pulses in the presence of very large overload pulses which makes it particularly useful for pulse height analysis of x rays in the presence of high energy gamma rays. The balance for low frequency components adjustment was adjusted, with the aid of an oscilloscope, for optimum performance. The overshoot was adjusted to less than one per cent to permit an energy less than 10 keV to be measured. A precision pulser and the 60 cycle noise component was used to make these adjustments with the oscilloscope (Tektronix Type 545A).

The single-channel pulse height analyzer is an instrument which generates an output pulse if and only if an input pulse has an amplitude falling between two preset voltages. Pulses of all other amplitudes are discarded. The difference between these two boundry voltages is called the channel width or window. The lower-level voltage is called the base line and may be adjusted to any voltage between zero and 100 volts, while the channel width is variable from zero to seven volts.

The single-channel analyzer is designed for high-resolution pulse-height analysis and uses the gain of an expander amplifier to reduce the drift in channel width to a neglible amount. The channel width varied about 0.5 per cent over the entire range and was checked by using a precision pulser. The input to the analyzer can be any pulse shape with a flat top of at least one microsecond. The output is negative and variable from 0 to 15 volts.

The decade scalar used in a Hamner (Type N-221) and is particularly suited for fast counting. The instrument has a dual low-level discriminator and can resolve pulses separated by one microsecond. The input is negative from -0.25 to -5.0 volts.

Experimental Method

The internal conversion coefficient of the K-shell can be measured by using a scintillation spectrometer. An atom, which has lost a K-electron due to the internal conversion process will emit K x rays. Thus with the scintillation spectrometer one can obtain a spectrum of a source with peaks corresponding to the gamma-ray and the x ray. Of course, the x ray must be of energy above the limit determined from the overshoot setting of the linear amplifier. That is the overshoot was adjusted to less than one per cent to permit an energy less than 10 keV to be measured. Using the following methods it is possible to measure the relative intensity of the gamma rays and that of the x ray (33). Hence, the internal conversion coefficient of the K shell can be determined.

The scintillation spectrometer used to determine the relative intensity of the gamma rays and that of the x ray consists of the

components previously described in the section on apparatus. block diagram is shown in Figure 7.

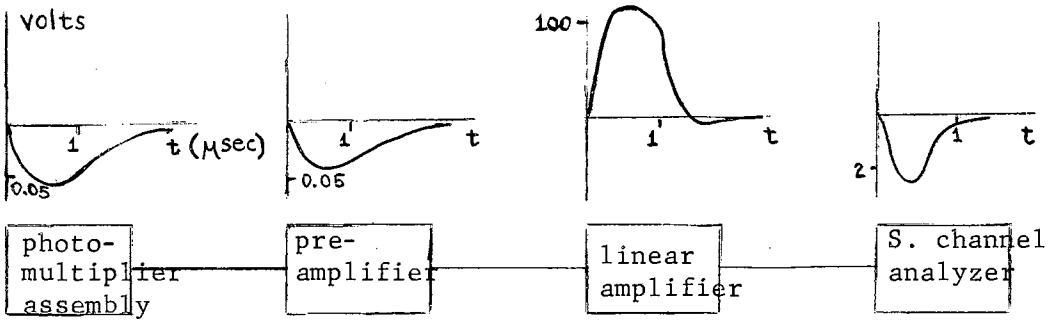

Figure 7. Typical Signals of the Spectrometer

The spectrometer was checked thoroughly using a precision pulser and an oscilloscope. Adjustments were made so as to have pulses of the desired shape for the best performance of the system. The shapes of these pulses can be seen in Figure 7. The output pulse of the photomultiplier is developed near ground potential so special precautions were taken on grounding the system. The system was checked for erratic counts (34) in the following way. Two counting rates were obtained by taking two ten minute counts of a source with a long half-life. The deviation is $\sigma = \left(\frac{r_1}{t_1} + \frac{r_2}{t_2}\right)^{\frac{1}{2}}$ and $k = \left(\frac{r_1}{t_1} - \frac{r_2}{t_2}\right)/\sigma$. Using this value of k and the tables (34), the probability of obtaining this difference because of statistical fluctuations is about 0.5. So it is quite certain the counter is not receiving erratic counts since a probability as low as 0.1 would also indicate that the counter was not receiving erratic counts.

The crystal and photomultiplier were both shielded. The crystal was shielded by approximately 2 inches of lead which was in the form of a hollow cylinder and enclosed the entire crystal. This lowered the counts due to the natural background. A "Chi-squared Test" was run

to evaluate the probability that the background readings follow the gaussian distribution (35). The quantity χ^2 is defined as,

$$\chi^2 = \sum_{i=1}^{n} \frac{(\bar{n}-n_i)^2}{\bar{n}} .$$

Thirty-five ten minute readings of background were taken and a value of χ^2 was calculated to be 32.916. From the tables (36) a value of 0.6 was obtained for the probability that the distribution is gaussian.

The spectrometer was calibrated using Co^{60} and Cs^{137} sources. The instrument was very nearly linear at energies above 1 MeV, but the small energy peaks were slightly shifted toward higher energies on the base line (37). This small non-linear effect seemed to be characteristic of the 6292 tube.

It was found that many things affect the resolution of the spectrometer, among these are: crystal fluorescent efficiency, light collection efficiency, photocathode efficiency and uniformity, photo-electron collection efficiency, multiplication effect (38), space charge limitation, amplifier noise and predifferentiator non-linearity, photo-multiplier noise, and fatigue effects. The effects that were found to be most importnat and could be corrected most readily were space charge limitation, amplifier noise and predifferentiator non-linearity. The RC value at the output of the photomultiplier was determined to give a pulse which was of duration suitable to the amplifier. It was found that staggering the resistances at the last three dynodes and plate with small capacitances added between these last three dynodes improved the resolution of the instrument. A variable resistance was added between the last dynode and the plate which could be adjusted for best resolution and cut down any secondary emission that might occur.

After the spectrometer was adjusted for the best resolution that could be obtained, spectra such as that shown in Figure 13 could be measured. For a source such as Cs^{137}, where only one gamma ray is emitted, the K-shell internal conversion coefficient is relatively easy to determine. From a scintillation spectrum this can be done by comparing the gamma and x ray intensities as follows: $\alpha_K = N_x/N_\gamma\omega_K = S_x\epsilon_\gamma/S_\gamma\epsilon_x\omega_K$ where S_γ and S_x are the areas under the gamma and X-ray photopeaks in the scintillation spectrum. These areas can be found by using Simpson's rule for irregular areas. The value for ω_K, the fluorescent yield for the K-shell can be found in the tables (39). ϵ_x and ϵ_γ are the efficiencies for the x and gamma ray respectively. The efficiency is defined as the ration N_{ph}/N_{total} where N_{ph} is the number of pulses under the photopeak and N_{total} is the total number of quanta of corresponding energy entering the crystal. The efficiency depends very strongly on the energy and for low energy the efficiency is practically 100 per cent. By using sources which were calibrated, the efficieny could be determined from a knowledge of the source distance and dimensions of the crystal. The efficiency can also be found by a method described by Lazar, Davis and Bell (40). Using this method, the peak efficiency, ϵ_p of a scintillation spectrometer is defined as the probability that a gamma ray of energy E will cause a pulse that will fall in the full-energy peak if it strikes the crystal. Thus, the intensity of the gamma ray of energy E is related to the area under the full-energy peak by the peak efficiency and solid angle. Because of the high probability for multiple collisions in the crystal, it is difficult to calculate ϵ_p directly. However, it is relatively easy to calculate ϵ_t, the total efficiency of the crystal for a gamma ray of

energy E. Then ϵ_p can be determined by a measurement of R, the ratio of the area under the full-energy peak to the area under the total spectrum. The peak efficiency is then, $\epsilon_p = R\epsilon_t$.

Evaluation of R by experiment can easily lead to an erroneous result if considerable caution is not taken. The major difficulty lies in determining accurately the total spectrum of only a single incident gamma ray. The low energy portion of the spectrum is most likely to be in error due to noise and in correct location of the origin (zero energy). In Figure 8 the full energy peak is represented by the cross-hatched area and the total spectrum by the sum of the shaded areas.

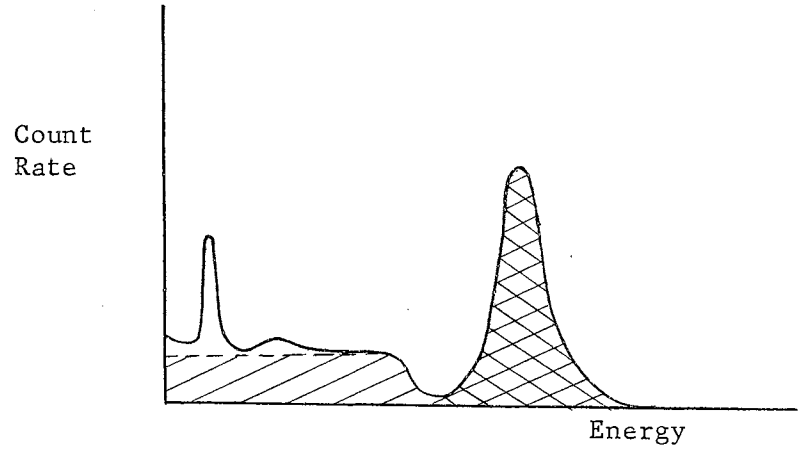

Figure 8. Typical Areas under the Photo Peak and the Total Spectrum.

The Monte Carlo method (41) has been used to calculate the peak efficiencies. In this computation, the computer simulates the physical processes which would take place in the crystal due to interactions of an individual incident photon. The interactions are followed until all the photon energy is lost in the crystal or a photon escapes from the crystal. The values obtained by these calculations are somewhat

higher than those obtained from the methods previously described.

The x ray photo peaks are attenuated by the amount of air between the source and the crystal and the backcap of the crystal. Weak sources were used so that the source could be placed on top of the crystal doing away with the attenuation by air, but corrections must be made for the attenuation by the aluminum foil backcap. The mass attenuation coefficient can be determined experimentally by using the x ray peak and sheets of aluminum foil of the correct thickness. Since the thickness of the aluminum foil backcap is known, the amount of attenuation can easily be determined. The experimental value of the mass attenuation coefficient was found to be less than the value given by the tables, because a collimated beam was not used to obtain the experimental value; however the uncollimated value fits our experimental situation. The x ray of low energy must be pulled away from the region of noise and dark current and this is accomplished by increasing the gain of the linear amplifier. In order to see how the area under the x ray peak behaved after an increase in gain, the area under the 32 keV x ray was determined at different settings of gain. Thus a correction of the x ray peak area could be made if an increase in amplification were necessary. The 32 keV x ray was well defined without an increase in amplifier gain and could be separated from the background due to the Compton continua very easily. An indication of how the separation from the background should be done was obtained by looking at the scintillation spectrum of Cs^{131} which emits only X-rays (42). Using this indication the x ray peak can be separated from the background with the needed precision.

For the case of complex spectra such as that of Co^{60}, the complex

gamma spectra can be analyzed into components by successively subtracting the single spectra due to the highest energy gamma ray (43). The analysis into the components was performed in the following way: The Compton distributions were determined experimentally for Cs^{137} and Na^{22}. These scintillation spectra were plotted on a scale such that, the theoretical compton edges (computed from the energy of the gamma ray) coincide and the heights of the photopeaks become equal (Figure 9). An unknown Compton continuum such as that for the 1.33 MeV gamma ray of Co^{60} can be obtained with a precision of about three per cent by graphical interpolation. This is easily done since the counting rates and pulse heights are plotted logarithmically and the photopeak can be brought into the correct position by simply shifting the curve as a whole.

After the complex spectra has been separated into single gamma ray photopeaks and their associated spectra, the peak efficiency can be found by the method previously described. However, the peak efficiency will be decreased since the two gamma rays are in cascade and a third peak in the spectrum is possible (coincident sum peak) when both gamma rays are completely absorbed (44) in the crystal. This effect was found to be negligible in the case of Co^{60}. The K-shell internal conversion coefficients can be determined just as the case of one gamma ray previously described. However, the x ray peak is now the sum of the x ray peaks due to the internally converted gamma rays. To determine the area under each of the x ray peaks, a ratio of the theoretical values of the K-shell internal conversion coefficients can be used. Thus, for Co^{60}

$$\frac{S_X^{1.17}}{S_X^{1.33}} = \frac{S_\gamma^{1.17} e_\gamma^{1.33}}{S_\gamma^{1.33} e_\gamma^{1.17}} \frac{\overline{\alpha_K^{1.17}}}{\overline{\alpha_K^{1.33}}}$$

where $\overline{\alpha_K^{1.17}}$ and $\overline{\alpha_K^{1.33}}$ are the mean possible theoretical values of Table II.

TABLE II

THEORETICAL VALUES OF α_K (10^4)

Energy (meV)	E 2^1	E 2^2	E 2^3	M 2^1	M 2^2
1.17	0.72	1.55	3.01	1.38	2.87
1.33	0.58	1.17	2.07	1.03	2.07

Since the area under the sum of the x ray peaks can be measured and corrected for attenuation and an increase in amplifier gain, the K-shell internal conversion coefficients can be found.

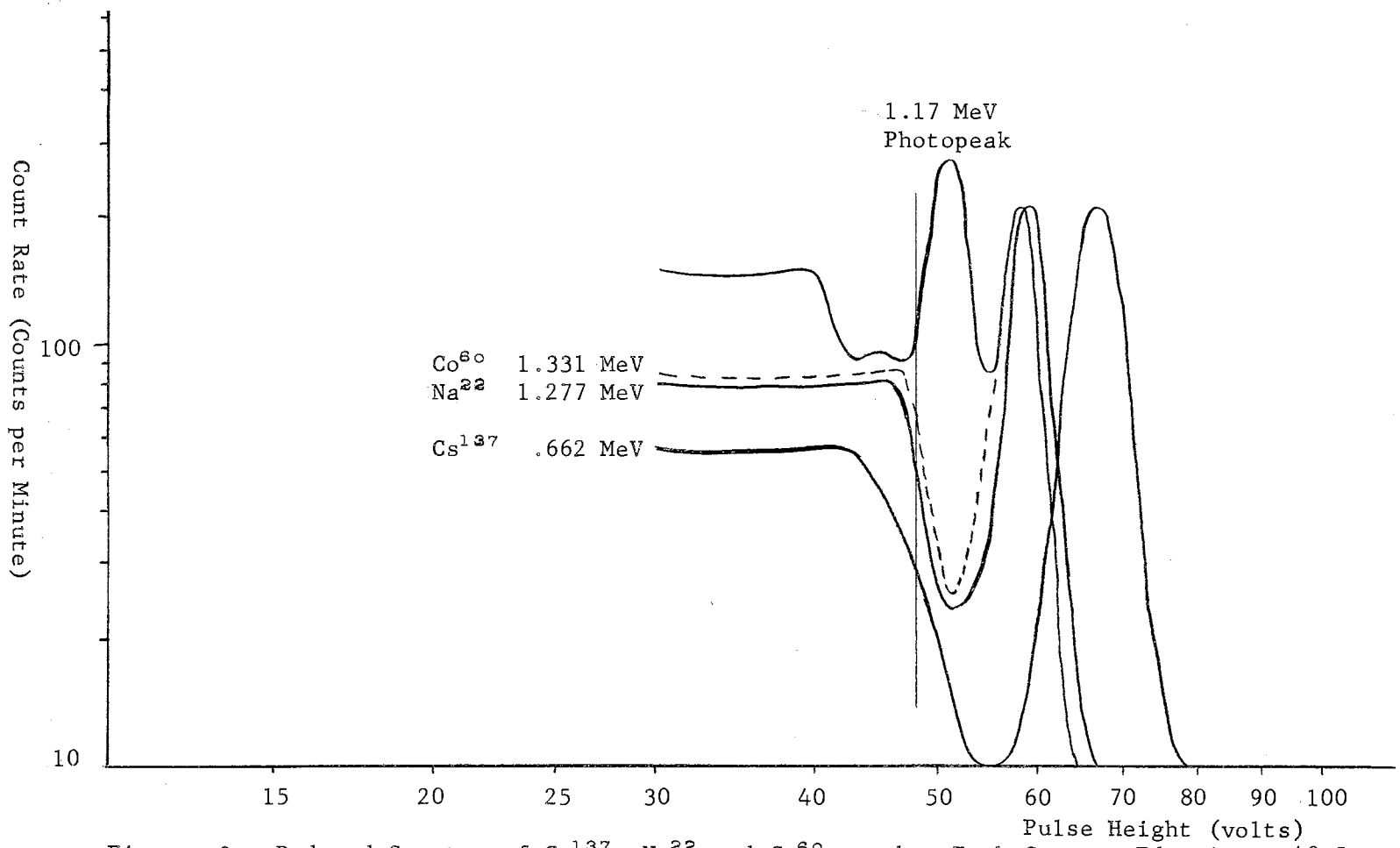

Figure 9. Reduced Spectra of Cs^{137}, Na^{22} and Co^{60} so that Each Compton Edge is at 48.5 and Each Photo Peak has the Same Height.

PRESENTATION OF DATA AND EXPERIMENTAL RESULTS

The following curves shown in Figures 10 through 16 were taken with the photomultiplier tube voltage at 700 volts and a 0.75 volt window on the single channel analyzer. These curves were corrected for background counts and the error bars were computed using the following relations,

$$\sigma = (\sigma_a^2 + \sigma_b^2)^{\frac{1}{2}}$$

where σ_a and σ_b are the standard deviations of the count rate with and without the sample. Since the background is small compared to the actual count rate, it is reasonable to assume that σ_b is negligible so that

$$\sigma \cong \sigma_a = (n)^{\frac{1}{2}}/t$$

where n is the number of counts and t is the time. So if n is the number of counts counted in a time interval t, the counting rate r is, $r = n/t$. This value with its standard deviation is,

$$r \pm \sigma_a = r \pm (r/t)^{\frac{1}{2}}$$

or in terms of per cent error we have

$$r \pm \frac{100\%}{(rt)^{\frac{1}{2}}} = r \pm \frac{100\%}{(n)^{\frac{1}{2}}}$$

Therefore each point in the curves was determined by taking a large number of counts. The number of counts at the lower points in the curves was greater than 1100 so as to have the standard error less than three per cent in any case. In most cases ten minute readings were sufficient but some of the lower points required longer counting times.

The measurements for Cs^{137} are shown in Figures 10 through 12. The areas under these curves were determined by using Simpson's rule for irregular areas and corrected for background and attenuation. These values along with values from the tables which will be used to determine the K-shell internal conversion coefficient are listed in Table III.

TABLE III

VALUES USED TO DETERMINE α_K FOR Cs^{137}

S_Y	S_x	S_t	R
2.22 (10^4)	6.16 (10^4)	4.94 (10^4)	0.452
ω_K	ϵ_x	ϵ_t	ϵ_p
0.876	0.97	0.534	(a) 0.242 (b) 0.258

The value of ϵ_p in Table III designated by (b) is the value obtained by using the method described by Lazar, Davis and Bell and the one designated by (a) was obtained from the source strength, geometry and observed counting rate.

The data for the mass attenuation coefficient for photons in aluminum using the 32 keV x ray are shown in Figure 12. This yielded the experimental value 0.93 cm^2 per gram for the mass attenuation coefficient. This value is less than the value given in the tables since a collimated beam was not used to determine the experimental value. The area of the x ray peak was corrected using the experimental value and the K-shell internal conversion coefficient for Cs^{137} was found to be 0.099 ± 0.010.

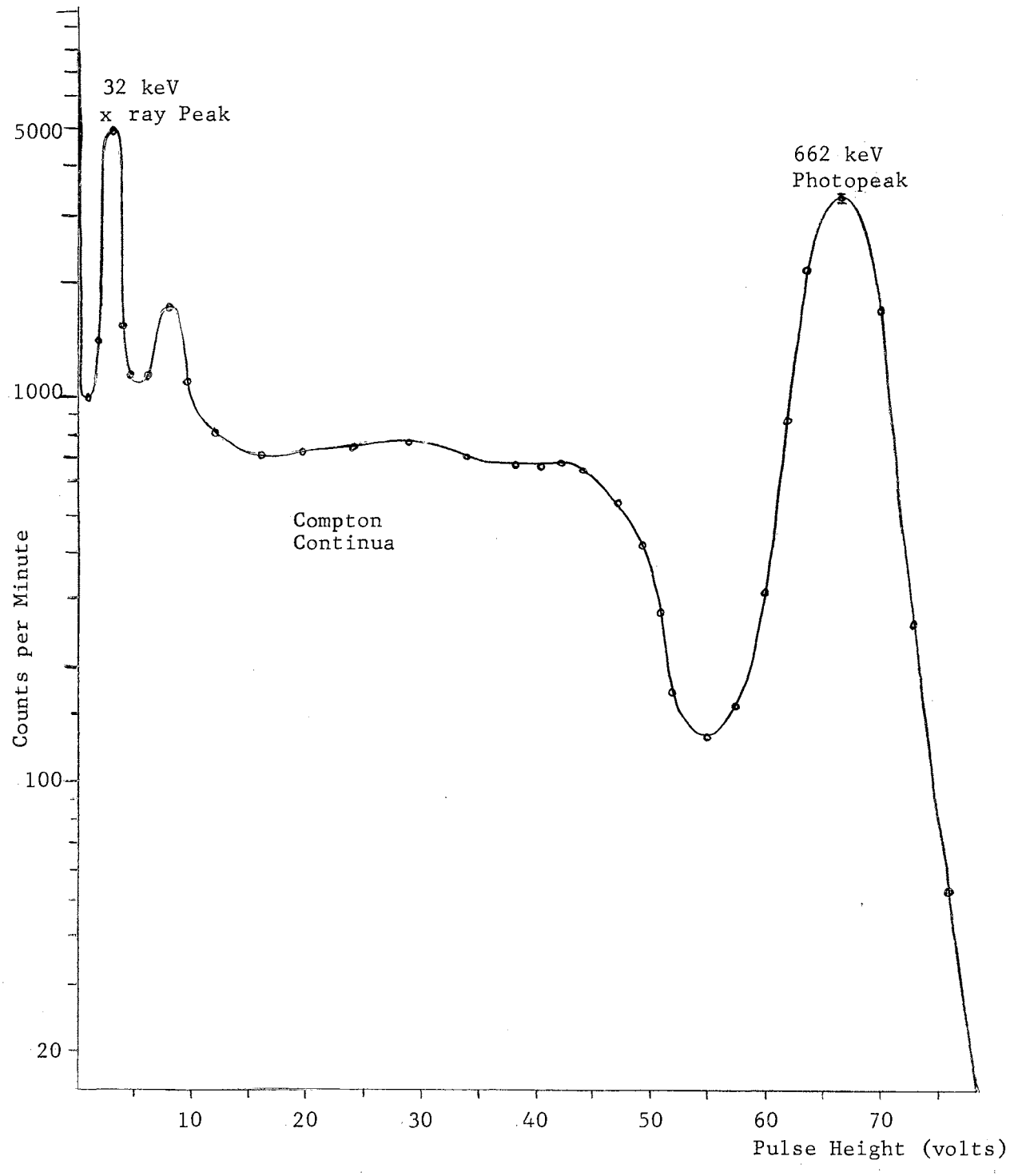

Figure 10. Scintillation Spectrum of Cs^{137} with the Amplifier Gain at 3200

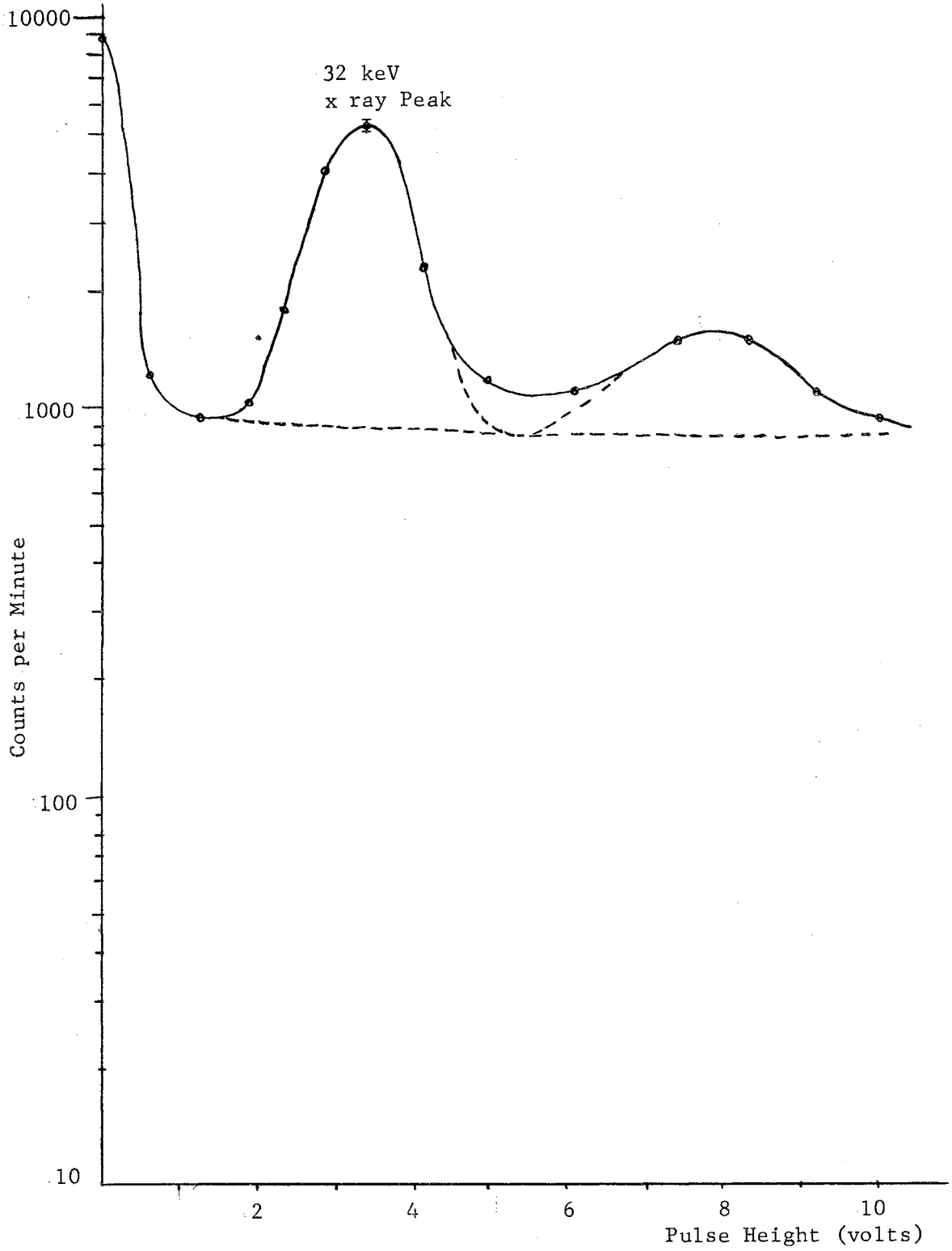

Figure 11. Spectrum showing the 32 keV x ray with the Amplifier Gain at 3200.

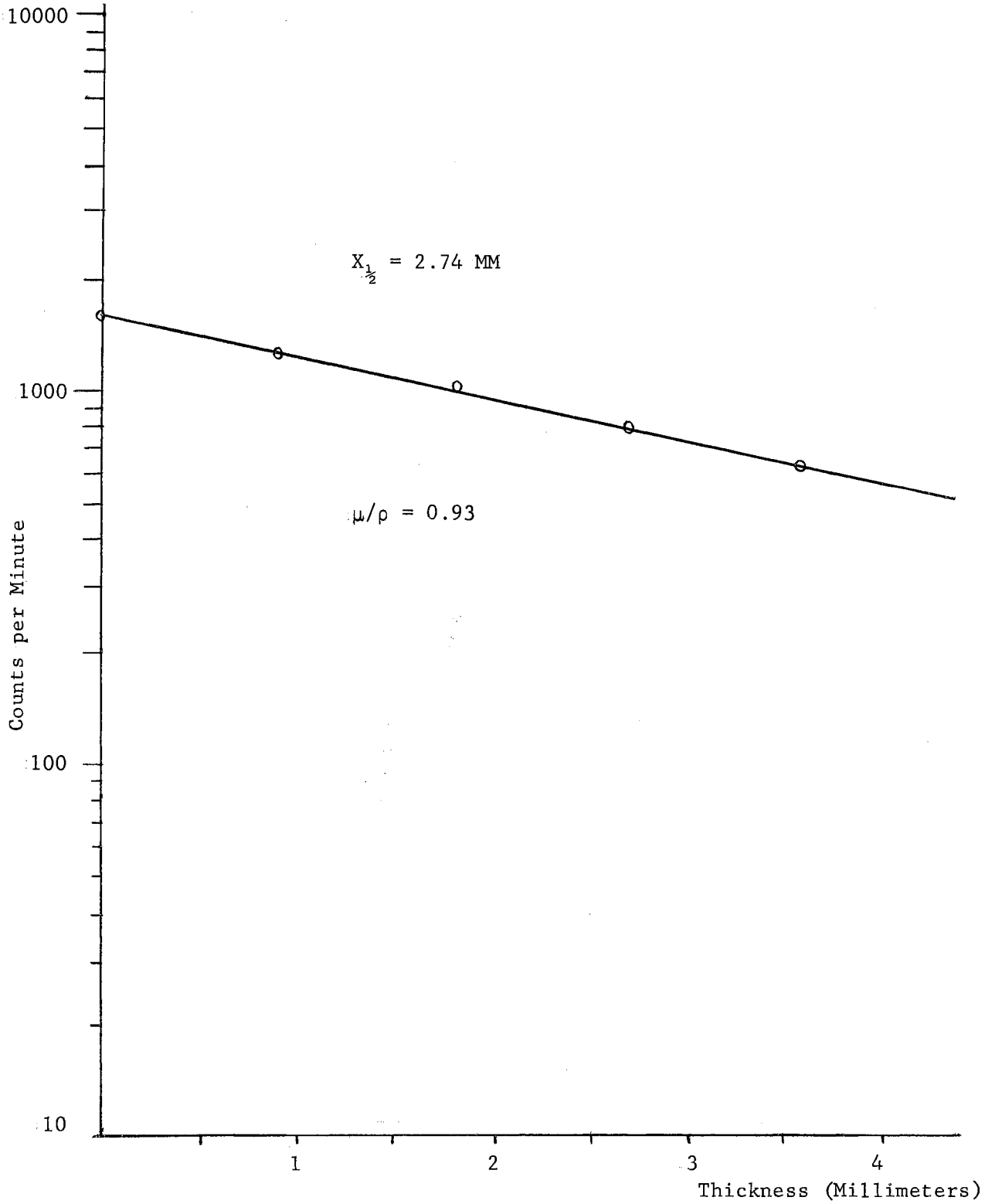

Figure 12. Mass Attenuation Coefficient for Aluminum using the 32 keV x ray

Figure 13 shows the scintillation spectrum of Co^{60} which was obtained using an amplifier gain of 2140. A resolution of 6.1 per cent was obtained for the 1.33 MeV gamma ray photopeak and a resolution of 6.7 per cent for the 1.17 MeV gamma ray photopeak. This resolution was obtained by taking the width of the photopeak at half the maximum counting rate for the position of the photopeak on the base line. The 1.33 MeV gamma ray photopeak and its associated features was subtracted from the total spectrum as indicated in Figure 11. The treatment then was essentially that for two single gamma ray spectra and yielded the areas that are given in Table IV. The x ray photopeak shown in Figure 14 was obtained by using an amplifier gain of 6400. The area of this peak is small and long counting times were used to have the needed accuracy for the points of the peak and those of the surrounding background. Figure 16 shows the relative position of the 32 keV x ray peak at the same settings of the spectrometer for which the Ni^{60} x ray was obtained. These positions indicate a slightly higher energy for both x rays and seemed to be characteristic of the photomultiplier tube.

The Ni^{60} x ray was used to determine the mass attenuation coefficient for photons in aluminum as shown in Figure 15. These measurements yielded an experimental value of 30.4 cm^2 per gram for the mass attenuation coefficient. This experimental value is then used to correct the area under the x ray photopeak as given in Table IV. This value of the area was also corrected for the increase in amplifier gain and represents the sum of the areas of the x ray peaks due to both internally converted gamma rays.

TABLE IV

VALUES USED TO DETEMINE α_K FOR Co^{60}

$S_V^{1.17}$	$S_V^{1.33}$	S_X	$S_t^{1.17}$
8.235 (10^3)	6.79 (10^3)	27	5.20 (10^4)

$S_t^{1.33}$	$e_p^{1.17}$	$e_p^{1.33}$	$R^{1.17}$	$R^{1.33}$	ω_K
5.39 (10^4)	3.8 (10^{-2})	2.8 (10^{-2})	1.58 (10^{-2})	1.26 (10^{-2})	3.26 (10^{-2})

Using the mean possible theoretical values of the internal conversion coefficients from Table II and the relation,

$$S_X = S_X^{1.17} + S_X^{1.33} = 27$$

we have,

$$S_X^{1.17} = 14.8 \text{ and } S_X^{1.33} = 12.2.$$

Now using these values for the areas of the x ray peaks along with the values of Table IV, the following values were determined for the K-shell internal conversion coefficients,

$$\alpha_K^{1.17} = 2.08 \pm 0.18 \ (10^{-4})$$

and

$$\alpha_K^{1.33} = 1.55 \pm 0.14 \ (10^{-4}).$$

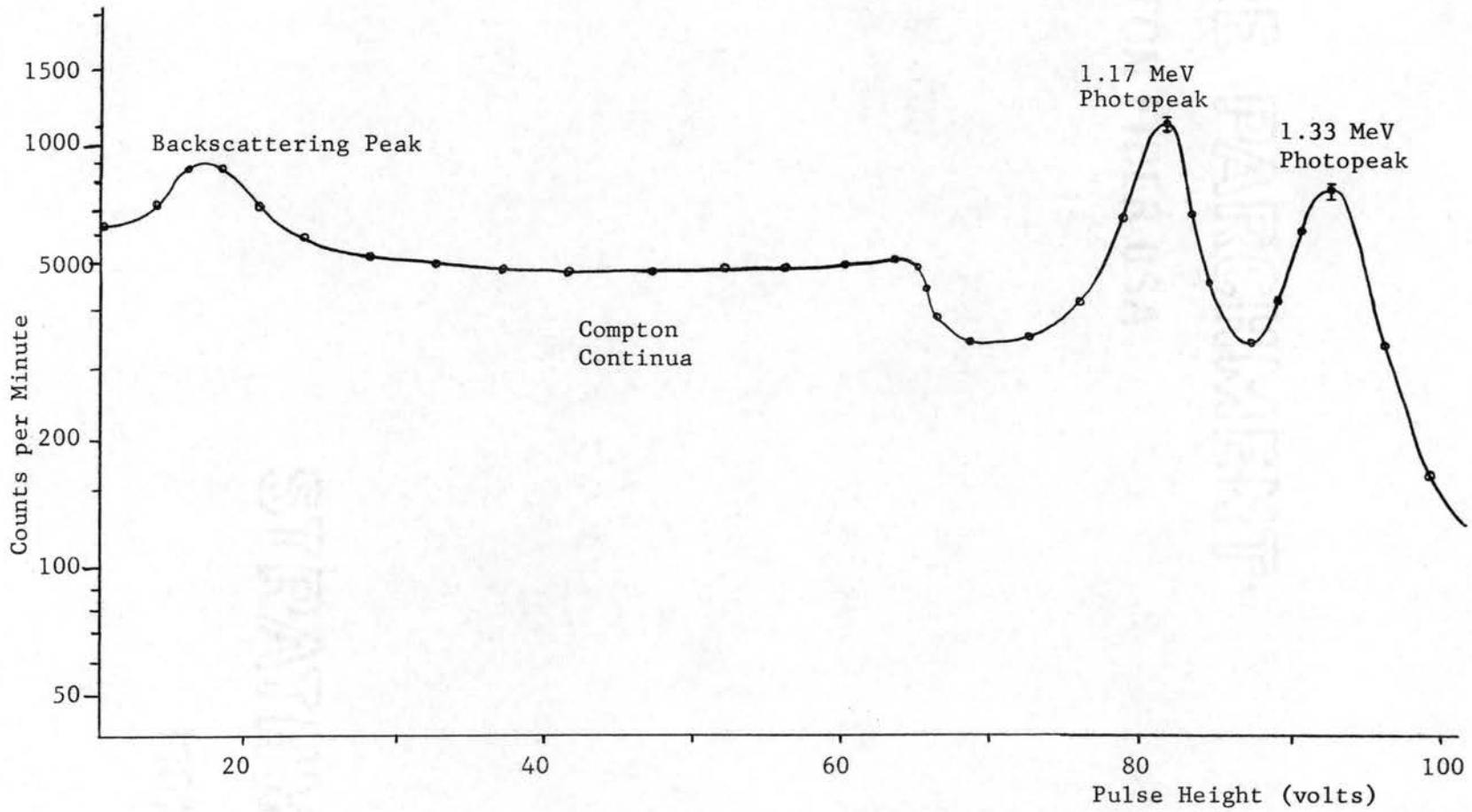

Figure 13. Scintillation Spectrum of Co^{60} with the Amplifier gain at 2140

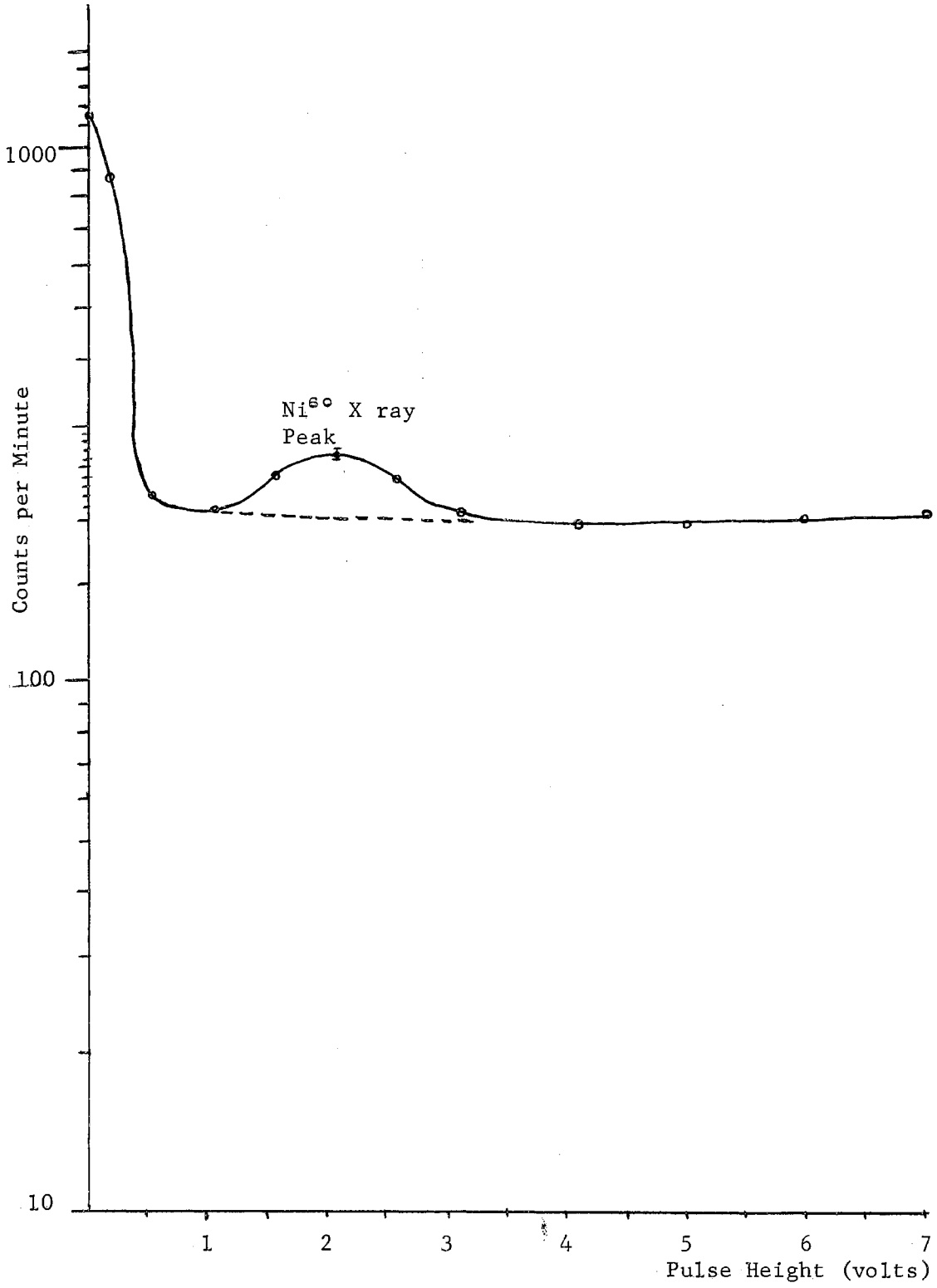

Figure 14. Spectrum Showing the Ni^{60} X ray at an Amplifier Gain of 6400

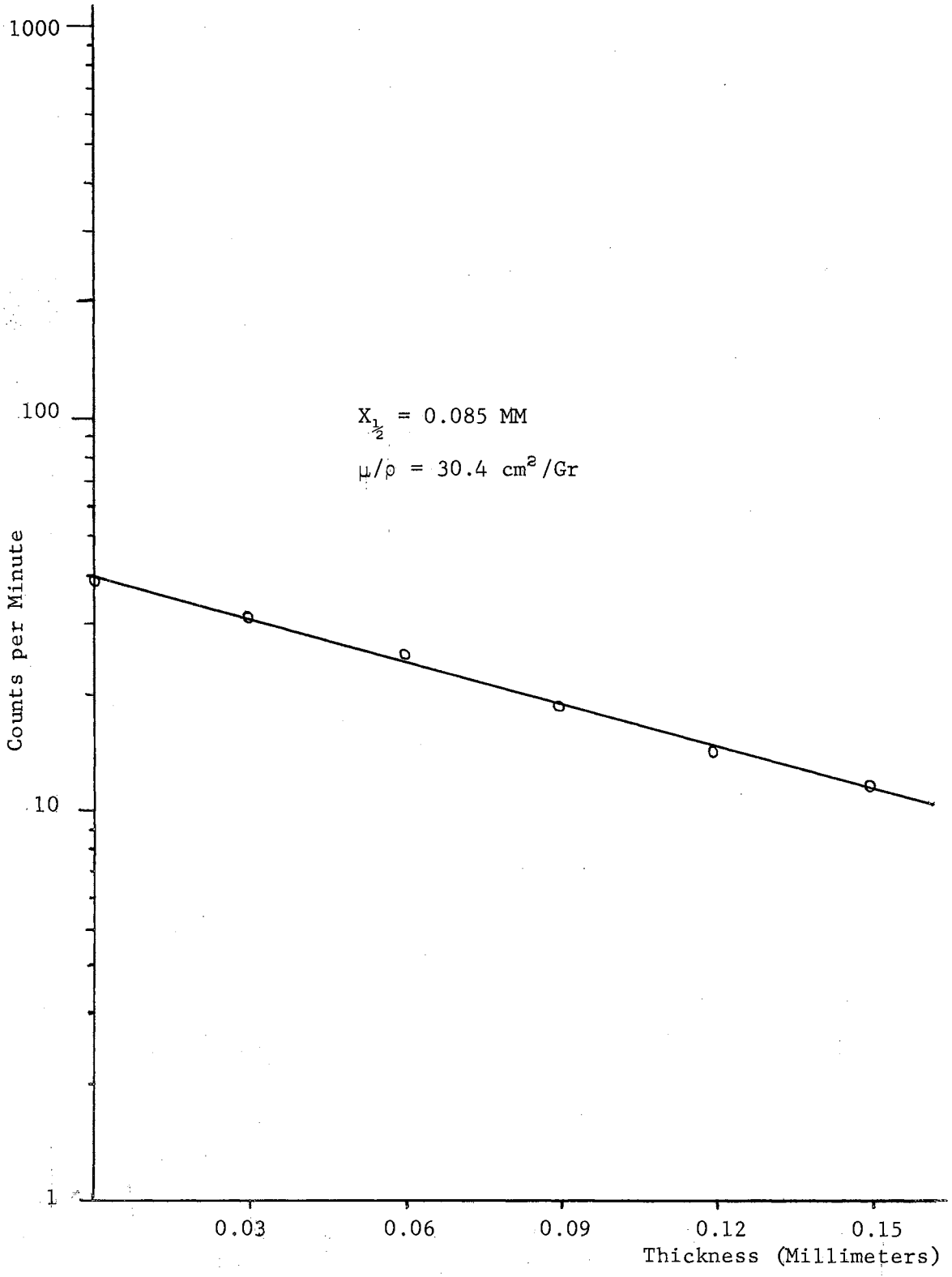

Figure 15. Mass Attenuation Coefficient for Aluminum using the Ni^{60} X ray

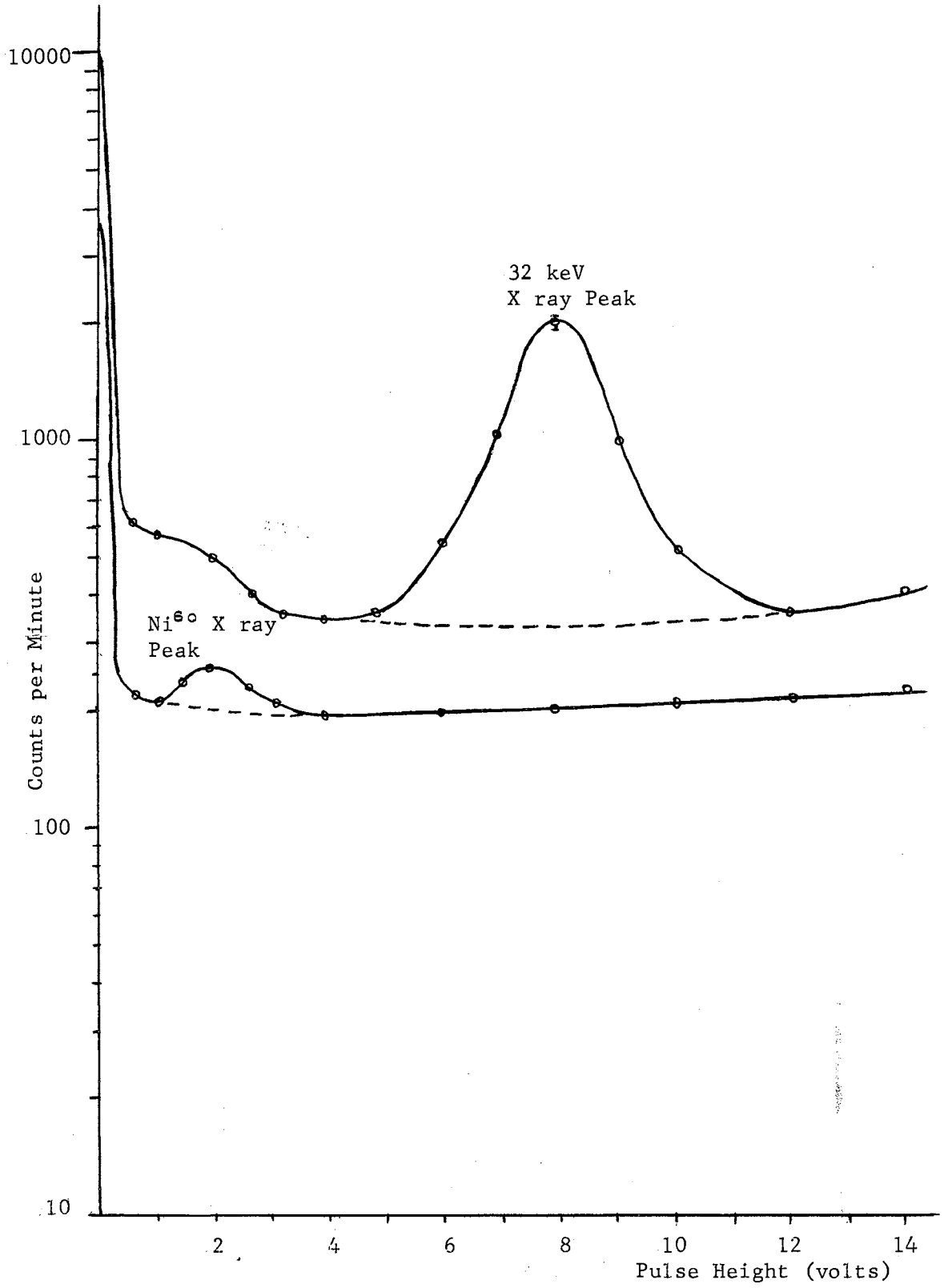

Figure 16. Comparison of the Positions of the X ray Peaks with the Amplifier Gain at 6400

DISCUSSION AND CONCLUSIONS

For a gamma ray of electric or magnetic multipole radiation, the following two selection rules must be obeyed in the gamma transition: (1) The photon which is emitted from a 2^L electric or magnetic multipole has angular momentum $L\hbar$ with respect to the position of the multipole. Thus, if I and I' are the angular momenta in units of $\hbar$ of the initial and final states of the radiating system, then L must have the value $|I - I'| \leq L \leq |I + I'|$ with the lowest value of L most probable. (2) This selection rule governs the parity change between initial and final states. Electric 2^L-pole or magnetic 2^L-pole radiation occurs only between states of the same parity if L is even and only between states of opposite parity if L is odd.

The K-shell internal conversion coefficient for Cs^{137} was found to be 0.099, which agrees with the theoretical value for magnetic 2^4-pole radiation. Now it is known that the spins of the ground states of Cs^{137} and Ba^{137} are 7/2 and 3/2, respectively, and that Cs^{137} decays by beta emission either to the ground state of Ba^{137} or to an excited state of Ba^{137}, which then decays by single gamma ray emission to the ground state of Ba^{137}. This gamma ray is highly internally converted (45, 46). It can be assumed that the ground state of Ba^{137} has even parity as predicted by the nuclear shell model (47). Now from the work of Langer and Moffat (48), $\Delta I = \pm 2$ and there is a change in parity. Since the gamma ray is magnetic 2^4-pole radiation, the selection rule obeyed in the gamma transition is $|I - I'| \leq 4 \leq |I + I'|$. The parity

of the Ba^{137} excited state must be odd and the spin I must satisfy the condition $|I - 3/2| \leq 4 \leq |I + 3/2|$. Thus, the spin I of the Ba^{137} excited state must be 11/2 as indicated in the decay scheme of Figure 17. An assignment of 9/2 to this state can be ruled out since this would permit electric 2^3-pole radiation and the internal conversion coefficient would be much different from the experimental value.

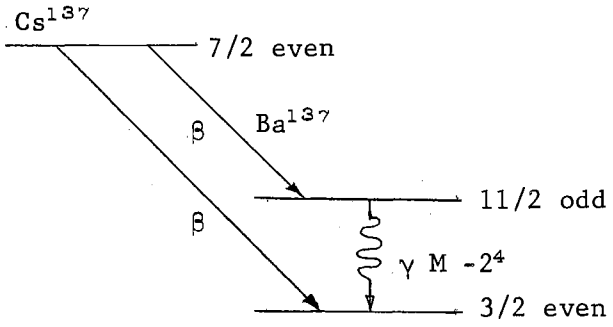

Figure 17. Decay Scheme of Cs^{137}

The K-shell internal conversion coefficients for Co^{60} were found to be $\alpha_k^{1.17} = 2.08\ (10^4)$ and $\alpha_k^{1.33} = 1.55\ (10^4)$. These measurements agree with those obtained by other methods given in Table I. The values indicate that both the gamma rays of Co^{60} are electric quadrupole (2^2-pole) radiations. This agrees with the angular correlation measurement (49) and the polarization-direction correlation measurement (50) which assigned the states of Ni^{60} involved in the decay of Co^{60} as 0, 2, and 4, respectively. Thus with the measurement of the internal conversion coefficients for the two gamma rays, the type of radiation is determined and the parities of the nuclear levels relative to each other can be fixed. It can be assumed that the ground state for Co^{60} has spin 5 and even parity since this is predicted by the nuclear shell model and is not inconsistant with the results. From the ratio

of the two conversion coefficients it is quite certain that the two gamma rays have the same parity, for example, if one of them is a magnetic quadrupole having odd parity, the other cannot be an electric quadrupole having even parity but could be either magnetic quadrupole or electric octupole.

The selection rules for electric quadrupole radiation are $|I - I'| \leq 2 \leq |I + I'|$ and no parity change. Comparison of the results with the angular correlation and polarization measurements fixes the spins and parities of the three Ni^{60} nuclear levels involved in the decay of Co^{60} as 0, 2 and 4 with all three levels having even parity as shown in Figure 20.

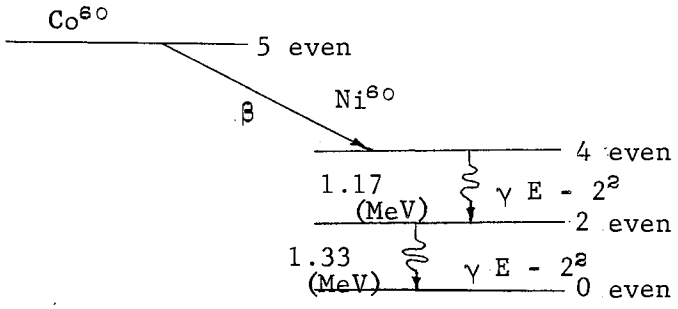

Figure 18. Decay Scheme of Co^{60}

At present, the scintillation spectrometer is not a high resolution device. Little improvement in resolution has been made in the past six years. If any improvement is to be made in this respect, the most likely source will be higher efficiencies in converting kinetic energy of electrons to light in the crystal and in the conversion of light back to electrons at the photocathode. Perhaps the answer to the problem of resolution lies in a device called the crystal conduction counter. In such a counter, following the interaction of the incident radiation with the crystal, an electric pulse is sensed directly as at a

boundary of the crystal. The energy transfers mentioned in the scintillation process are eliminated. The idea of the crystal conduction counter has been around for a number of years and the inherently better energy resolution of this counter has never been achieved in practice. The experimental difficulties that have prevented the general application of this type of counter have been reviewed by Hofstadter (51).

BIBLIOGRAPHY

1. Rose, M. E. "Theory of Internal Conversion." Beta- and Gamma-Ray Spectroscopy, Ed. K. Siegbahn. New York: Interscience Publishers Inc., 1955, pp. 398-413.

2. Evans, R. D. The Atomic Nucleus. New York: McGraw-Hill Book Company Inc., 1955, pp. 218-229.

3. Burhop, E. H. S. "Fluorescent Yield of the K-Shell." J. Phys. Radium, 16 (1955), 625.

4. Roos, C. E. "K Fluorescence Yield of Several Metals." Phys. Rev., 105 (1957), 931.

5. Hagedoorn, H. and A. H. Wapstra. "Branching Ratios of Electron Capture to Positron Emission." Nuclear Physics, 9 (1958), 296.

6. Burhop, E. H. S. The Auger Effect and Other Radiationless Transitions. London: Cambridge University Press, 1952.

7. Schafroth, R. "Koeffizienten der Inneren Konversion fur Magnetische Multipolstrahlung." Helv. Phys. Acta., 21 (1948), 499.

8. Lowin, I. S. and N. Tralli. "Magnetic Multipole Internal Conversion." Phys. Rev., 75 (1949), 529.

9. Griffith, B. A. and J. P. Stanley. "On the Numerical Calculation of the Internal Conversion in the K-Shell." Phys. Rev., 75 (1949), 534.

10. Rose, M. E. and G. Goertzel. "The K-Shell Internal Conversion Coefficients." Phys. Rev., 76 (1949), 184.

11. Austern, N. and R. G. Sachs. "Interaction Effects on Radiative Transitions in Nuclei." Phys. Rev., 81 (1951), 710.

12. Sliv, L. A. and I. M Band. Coefficients of Internal Conversion of Gamma Radiation. Moscow: U.S.S.R. Academy of Sciences, 1956.

13. Griffith, B. A. and J. P. Stanley. "On the Numerical Calculation of the Internal Conversion in the K-Shell." Phys. Rev., 75 (1949), 1110.

14. Fisk, J. B. and H. M. Taylor. "The Internal Conversion of Gamma Rays." Proc. Roy. Soc. (London), A 146 (1934), 178.

15. Reitz, J. R. "The Effect of Screening on Beta-Ray Spectra and and Internal Conversion." Phys. Rev., 77 (1950), 10.

16. Rose, M. E., G. Goertzel, and B. I. Spinrad. "The Internal Conversion Coefficients. I: The K-Shell." Phys. Rev., 83 (1951), 79.

17. Deutsch, M. and K. Siegbahn. "Internal Conversion in Ni^{60}," Phys. Rev., 77 (1949), 680.

18. Waggoner, M., A. Roberts, and P. B. Moon. "Internal Conversion of Gamma-Rays From Co^{60}, Cs^{134}, and Zn^{65}." Phys. Rev., 80 (1950), 420.

19. Fan, C. "Beta-Spectra and Internal Conversion Coefficients for Co^{60}, Nb^{95}, Au^{198}, and Hf^{181}." Phys. Rev., 87 (1952), 252.

20. Maeder, D. "On the Line Shape of a Gamma-Ray Scintillation Spectrometer." Helv. Phys. Acta., 27 (1954), 3.

21. Wapstra, A. H., G. Nijgh, and R. Van Lieshout. Nuclear Spectroscopy Tables. Amsterdam: North-Holland Publishing Company, 1959, p. 129.

22. Curran, S. C. Luminescence and the Scintillation Counter. New York: Academic Press Inc., 1953, pp. 72-75.

23. Price, W. J. Nuclear Radiation Detection. New York: McGraw-Hill, 1958, pp. 170-171.

24. Seitz, F. The Modern Theory of Solids. New York: McGraw-Hill, 1940, Chapter 13, p. 526.

25. Birks, J. B. Scintillation Counters. London: Pergamon Press, 1960, pp. 47-49.

26. Schiff, L. I. Quantum Mechanics. New York: McGraw-Hill, 1949, pp. 189-215.

27. Rose, M. E. Multipole Fields. New York: John Wiley and Sons, 1955, pp. 54-58.

28. Tralli, N. and G. Goertzel. "Theory of Internal Conversion." Phys. Rev., 83 (1951), 399.

29. Taylor, H. M. and N. Mott. "On the Interaction of Two Particles." Proc. Roy. Soc. (London), A142 (1933), 215.

30. Dancoff, S. M. and P. Morrison. "The Calculation of Internal Conversion Coefficients." Phys. Rev., 55 (1939), 122.

31. Church, E. L. and J. Weneser. "Effect of Finite Nuclear Size on Internal Conversion." Phys. Rev., 104 (1956), 1382.

32. Nilsson, S. G. and J. Rasmussen. "On Anomalous Conversion Coefficients of Dipole Transitions." Nuclear Physics. 5 (1958), 617.

33. Hofstader, R. and J. A. McIntyre. "The Measurement of Gamma-Ray Energies with Single Crystals of NaI(Tl)." Phys. Rev., 80 (1950), 631.

34. Price, W. F. Nuclear Radiation Detection. New York: McGraw-Hill, 1958, pp. 62-66.

35. Evans, R. D. The Atomic Nucleus. New York: McGraw-Hill Book Company Inc., 1955, pp. 775.

36. Fisher, R. A. Statistical Methods for Research Workers. New York: Hafner Publishing Company., 1950, pp. 112.

37. Nussbaum, R. H. "Nuclear Levels in Ni^{60} from the Decay of Cu^{60}." Physica, 20 (1954), 555.

38. Morton, G. A. "Two New Photomultipliers for Scintillation Counting." Nucleonics, 10 (1952), 44.

39. Wapstra, A. H., G. J. Nijgh, and R. Van Lieshout. Nuclear Spectroscopy Tables. Amsterdam: North-Holland Publishing Company, 1959, p. 81.

40. Lazar, N. H., R. C. Davis, and P. R. Bell. "Peak Efficiency of NaI." Nucleonics, 14 (1956), 52.

41. Crouthamel, C. E. Applied Gamma-Ray Spectrometry. New York: Pergamon Press Inc., 1960, pp. 107-108.

42. Bergstrom, I., S. Thulin, A. Wapstra, and B. Astrom. "Calibration of a Scintillation Spectrometer." Arkiv For Fysik, 7 (1953), 247.

43. Maeder, D., A. H. Wapstra, G. Nijgh, and L. Ornstein. "The Even Mass Isomers of Lead." Physica, 20 (1954), 521.

44. Rose, M. E. "The Analysis of Angular Correlation and Angular Distribution Data." Phys. Rev., 91 (1953), 610.

45. Davis, L. "Nuclear Spin and Magnetic Moment of Cs^{137}." Phys. Rev., 76 (1949), 435.

46. Davis, L., D Nagle, J. R. Zacharias. "Atomic Beam Magnetic Resonance Experiments with Radioactive Elements Na^{22}, K^{40}, Cs^{135}, and Cs^{137}." Phys. Rev., 76 (1949), 1069.

47. Feenberg, E. and K. C. Hammack. "Nuclear Shell Structure." Phys. Rev., 75 (1949), 1877.

48. Langer, L. M. and R. Moffat. "The Twice-Forbidden Transition of Cs^{137}." Phys. Rev., 82 (1951), 333.

49. Brady, E. L. and M. Deutsch. "Angular Correlation of Successive Gamma Rays." Phys. Rev., 78 (1950), 558.

50. Metzger, F. and M. Deutsch. "Study of the Polarization-Direction Correlation of Successive Gamma Ray Quanta." Phys. Rev., 78 (1950), 551.

51. Hofstadter, R. "Crystal Counters." Nucleonics, 4 (1949), 2.

52. Morse, P. M. and H. Feshbach. Methods of Theoretical Physics. New York: McGraw-Hill, 1953, Chapter 9, p. 999.

53. Hulme, H. R. "The Interaction of Two Particles." Proc. Roy. Soc. (London), A154 (1936), 487.

54. Preston, M. A. Physics of the Nucleus. Reading, Massachusetts: Addison-Wesley Publishing Company, (1962), pp. 302-310.

APPENDIX A

EXPANSION OF THE RADIATION FIELD IN SPHERICAL HARMONICS

We can write the solution to the wave equation as ,

$$\varphi_L^M(kr) = k f_L(kr)\, Y_L^M(\theta,\varphi) \tag{A.1}$$

in which $f_L(kr) = (kr)^{-\frac{1}{2}} J_{L+\frac{1}{2}}(kr)$, where J is the bessel function and $Y_L^M(\theta,\varphi)$ is the normalized spherical harmonic. Now φ_L^M satisfies the equations

$$\nabla^2 \varphi_L^M - k^2 \varphi_L^M = 0 \quad , \quad \int d\tau\ \varphi_L^M(k)\ \varphi_{L'}^{M'*}(k') = \delta_{LL'}\delta_{MM'}\delta(k-k'), \tag{A.2}$$

It may be shown that the radiation potentials can be written as (52)

$$A_{LM}^{(l)} = \left(\frac{1}{k}\right)\nabla\varphi_L^M \tag{A.3}$$

$$A_{LM}^{(m)} = \left[L(L+1)\right]^{-\frac{1}{2}}(\vec{r}\times\nabla)\varphi_L^M \tag{A.4}$$

$$A_{LM}^{(e)} = \left[k^2 L(L+1)\right]^{-\frac{1}{2}}\nabla\times(\vec{r}\times\nabla)\varphi_L^M \tag{A.5}$$

in which the subscripts l, m, e, on the A_{LM} refer to longitudinal, magnetic and electric radiations, respectively.

Using the unit vectors

$$\vec{u}_1 = -2^{-\frac{1}{2}}(\hat{i} + i\hat{j}), \quad \vec{u}_0 = \hat{k}, \quad \vec{u}_{-1} = 2^{-\frac{1}{2}}(\hat{i} - i\hat{j})$$

such that all vectors may be written

$$\vec{V} = \sum_\sigma V_\sigma \vec{u}^\sigma = \sum_\sigma V^\sigma \vec{u}_\sigma$$

where $\vec{u}^\sigma = \vec{u}_\sigma^*$ and $V^\sigma = V_\sigma^*$ for a real vector, we may express the components of the A_{LM} as

$$A_{LM\sigma}^{(l)} = \left[\frac{L+1}{2L+1}\right]^{\frac{1}{2}}\left(M+\sigma,-\sigma|LM\right)_{L+1,1}\varphi_{L+1}^{M+\sigma} + \left[\frac{L}{2L+1}\right]^{\frac{1}{2}}\left(M+\sigma,-\sigma|LM\right)_{L-1,1}\varphi_{L-1}^{M+\sigma} \tag{A.6}$$

$$A_{LM\sigma}^{(m)} = i\left(M+\sigma,-\sigma|LM\right)_{L,1}\varphi_L^{M+\sigma} \tag{A.7}$$

$$A_{LM\sigma}^{(e)} = \left[\frac{L}{2L+1}\right]^{\frac{1}{2}}\left(M+\sigma,-\sigma|LM\right)_{L+1,1}\varphi_{L+1}^{M+\sigma} - \left[\frac{L+1}{2L+1}\right]^{\frac{1}{2}}\left(M+\sigma,-\sigma|LM\right)_{L-1,1}\varphi_{L-1}^{M+\sigma} \tag{A.8}$$

with the notation

$$\varphi_L^M(kr') = k\, J_L(kr')\, Y_L^M(\theta', \varphi')$$

$$\Psi_L^M(kr) = k\, H_L^{(1)}(kr)\, Y_L^M(\theta, \varphi)$$

$$I = \sum_\sigma \hat{u}_\sigma \hat{u}^\sigma \equiv \hat{\imath}\hat{\imath} + \hat{\jmath}\hat{\jmath} + \hat{k}\hat{k}$$

where $J_L(kr') = (kr')^{-\frac{1}{2}} J_{L+\frac{1}{2}}(kr')$, and $H_L^{(1)}(kr)^{-\frac{1}{2}} H^{(1)}_{L+\frac{1}{2}}(kr)$,

in which J is the bessel function and $H^{(1)}$ the hankel function of the first kind, the well known relation

$$\frac{e^{ikx}}{x} = i\pi(4rr')^{-\frac{1}{2}} \sum_L (2L+1) J_{L+\frac{1}{2}}(kr')\, H^{(1)}_{L+\frac{1}{2}}(kr)\, P_L(\cos\Theta)$$

where r is greater than r', $x = |r - r'|$, Θ is the angle between r and r', and

$$P_L(\cos\Theta) = \left[\frac{4\pi}{2L+1}\right] \sum_{M=-L}^{L} Y_L^{M*}(\theta', \varphi')\, Y_L^M(\theta, \varphi)$$

may be written

$$\left(\frac{e^{ikx}}{x}\right) I = \left(\frac{2\pi^2 i}{k}\right) \sum_{LM} \Psi_L^M\, \varphi_L^{M*} \sum_\sigma \hat{u}_\sigma \hat{u}^\sigma .$$

Introducing the vectors B_{LM} which bear the same relationship to Ψ_L^M as the A_{LM} to φ_L^M, it can be shown that (53) (p. 486)

$$\sum_{LMi} B_{LM}^{(i)}\, A_{LM}^{(i)*} = \sum_{LM} \Psi_L^M\, \varphi_L^{M*} \sum_\sigma \hat{u}_\sigma \hat{u}^\sigma$$

so that

$$\left(\frac{e^{ikx}}{x}\right) I = \left(\frac{2\pi^2 i}{k}\right) \sum_{LMi} B_{LM}^{(i)}\, A_{LM}^{(i)*}$$

Similarly,

$$\left(\frac{e^{-ikx}}{x}\right) I = -\left(\frac{2\pi^2 i}{k}\right) \sum_{LMi} B_{LM}^{(i)*}\, A_{LM}^{(i)} .$$

The radiation potentials in the different gauges are easily obtained. The equations of gauge transformation are

$$\varphi = \varphi' - \frac{d\lambda}{dt} , \qquad A = A' + \nabla\lambda \tag{A.9}$$

where λ is a solution of the wave equation $\nabla^2\lambda - \frac{d^2\lambda}{dt^2} = 0$.

In the Heitler gauge div A' = φ' = 0. Since the sole condition on λ is that it satisfy the wave equation, we may take $\lambda = \frac{1}{k} \varphi_L^M e^{-ikt}$

so that $\frac{d\lambda}{dt} = -i\,\varphi_L^M\, e^{-ikt}$, $\nabla\lambda = A_{LM}^{(l)}\, e^{-ikt}$,

$A' = A_{LM}^{(m)}\, e^{-ikt}$, or $A_{LM}^{(e)}\, e^{-ikt}$.

In this gauge, therefore, the expressions for φ and A are

$$i\,\varphi_L^M,\ A_{LM}^{(l)};\quad 0,\ A_{LM}^{(m)};\quad 0,\ A_{LM}^{(e)}.$$

The expressions for the scalar and vector potentials in the conventional gauge can be obtained. Take

$$\lambda = -\left[\frac{L}{k^2(L+1)}\right]^{\frac{1}{2}} \varphi_L^M\, e^{-ikt}$$

so that the scalar potential is

$$\varphi = -\frac{d\lambda}{dt} = -i\left[\frac{L}{L+1}\right]^{\frac{1}{2}} \varphi_L^M\, e^{-ikt}$$

and

$$\nabla\varphi = -\left[\frac{L}{L+1}\right]^{\frac{1}{2}} A_{LM}^{(l)}\, e^{-ikt}.$$

The electric multipole vector potential is then obtained from the equation of gauge transformation,

$$A^{(e)} = A_{LM}^{(e)} - \left[\frac{L}{L+1}\right]^{\frac{1}{2}} A_{LM}^{(l)}$$

The magnetic multipole vector potential remains as

$$A_{LM}^{(m)} = \left[\frac{L}{L+1}\right]^{-\frac{1}{2}} (\vec{r} \times \nabla)\, \varphi_L^M.$$

Hence in the conventional gauge there are no longitudinal potentials, and the electric multipoles have both scalar and vector potentials.

APPENDIX B

EVALUATION OF INTEGRALS

The Heitler gauge is used in the following calculations in order to simplify the evaluations as much as possible.

1. Evaluation of $U_{fo} = \int d\omega \left[\frac{H_{\varepsilon\omega} H_{\omega o}}{\omega - k - i\eta} + \frac{H'_{\varepsilon\omega} H'_{\omega o}}{\omega + \omega_o - i\eta} \right]$

Time-dependent perturbation theory tells us that the transition probility per unit time is appreciable only if energy is conserved between initial and final states (53). According to Schiff the second term in the integrand cannot be ignored. We can take it into account by integrating the first term from $-\infty$ to $+\infty$ instead of from 0 to $+\infty$.

Then
$$U_{fo} = \int_{-\infty}^{+\infty} d\omega \frac{H_{\varepsilon\omega} H_{\omega o}}{\omega - k - i\eta} = 2\pi e e' \sum_{LM;i} \int_{-\infty}^{+\infty} \frac{d\omega}{\omega(\omega - k - i\eta)} \tag{B.1}$$

$$\times \left\{ \int d\tau \, \psi_f^* \left[\alpha \cdot A_{LM}^{(i)}(kr) + i \varphi_L^{M(i)}(kr) \right] \psi_i \right\} \times \left\{ \int d\tau' \, \Phi_f^* \left[\alpha' \cdot A_{LM}^{*(i)}(kr') - i \, \varphi_L^{M(i)*}(kr') \right] \Phi_i \right\}$$

where the superscript (i) refers to the longitudinal, magnetic and electric 2^L multipole, and $\varphi_L^{M(i)} = 0$ for i = m, e and $\varphi_L^{M(q)} = \varphi_L^M$. The $\sum_{LM;i}$ of the bracketed terms may be written as

$$\sum_{LM;i} \int d\tau \int d\tau' \, \psi_f^* \Phi_f^* \left[\alpha \cdot A_{LM}^{(i)}(kr) \, \alpha' \cdot A_{LM}^{(i)*}(kr') + i \varphi_L^M(kr) \alpha' \cdot A_{LM}^{(q)*}(kr') \right.$$
$$\left. - i \varphi_L^{M*}(kr') \alpha \cdot A_{LM}^{(q)}(kr) + \varphi_L^M(kr) \varphi_L^{M*}(kr') \right] \psi_i \Phi_i . \tag{B.2}$$

Since the hamiltonians have the form,

$$H = -\alpha \cdot p - \beta m - \alpha \cdot A_{LM}^{(i)}(kr) - i \varphi_L^{M(i)}(kr)$$
$$H' = -\alpha' \cdot p' - \beta' m' - \alpha' \cdot A_{LM}^{(i)*}(kr) + i \varphi_L^{M(i)*}(kr')$$

we obtain $$\alpha \cdot A^{(\ell)}_{LM}(kr) = \left(\frac{1}{k}\right)\alpha \cdot \nabla \varphi^M_L(kr) = \left(\frac{i}{k}\right)\alpha \cdot p\, \varphi^M_L(kr)$$
$$= \left(\frac{i}{k}\right)\left[\varphi^M_L(kr)\, H - H\, \varphi^M_L(kr)\right]$$

and $$\alpha' \cdot A^{(\ell)*}_{LM}(kr) = \left(\frac{i}{k}\right)\left[\varphi^{M*}_L(kr) H' - H' \varphi^{M*}_L(kr')\right].$$

The (B.2) reduces to $$\int d\tau \int d\tau' \psi_f^* \Phi_f^* \left\{ \sum \alpha \cdot A^{(i)}_{LM}(kr)\, \alpha' \cdot A^{(i)}_{LM}(kr') + \left[1 - \frac{(W+E)}{k}\right] \sum_{LM} \varphi^M_L(kr)\, \varphi^{M*}_L(kr') \right\} \psi_i \Phi_i$$

Hence
$$U_{fo} = 2\pi e e' \int d\tau \int d\tau' \psi_f^* \Phi_f^* \left[\int_{-\infty}^{\infty} \frac{d\omega}{\omega(\omega - k - i\eta)} \times \left\{ \sum_{LMi} \alpha \cdot A^{(i)}_{LM}(kr)\, \alpha' \cdot A^{(i)*}_{LM}(kr') + \sum_{LM} \left[1 - \frac{W+E}{k}\right] \varphi^M_L(kr)\, \varphi^{M*}_L(kr') \right\} \right] \psi_i \Phi_i .$$

Now, the dependence of $\varphi^M_L(kx)$ and $A^i_{LM}(kx)$ on k is confined to the spherical bessel function $J_L(kx)$ which each contains. We will consider the case where r is greater than r' and make substitution, $2J_L(kr) = H^{(1)}_L(kr) + H^{(2)}_L(kr)$. The integral is to be evaluated for conservation of energy, that is, W = E = k = ω. Then, from the location of the pole, it is clear that only the $H^{(1)}_L(kr)$ part of $J_L(kr)$ will contribute to the integral. Therefore,

$$U_{fo} = \left(2\pi^2 e e' \frac{i}{\omega}\right) \int d\tau \int d\tau' \psi_f^* \Phi_f^* \left\{ \sum_{LMi} \alpha \cdot B^{(i)}_{LM}(\omega r) \times \alpha' \cdot A^{(i)*}_{LM}(\omega r') - \sum_{LM} \psi^M_L(\omega r)\, \varphi^{M*}_L(\omega r') \right\} \psi_i \Phi_i \qquad (B.3)$$

where the B_{LM} differs from the A_{LM} only in the replacement of J_L by $H^{(1)}_L$.

Now in general, the radiation field does not contain all the multipoles. The selection rules usually restrict the radiation field to a given multipole, say the 2^L-th, of a particular type (1, e or m). In this case (B.1) reduced to

$$U'_{fo} = 2\pi e e' \int_{-\infty}^{\infty} \frac{d\omega}{\omega(\omega - k - i\eta)} \int d\tau\, \psi_f^* \left[\alpha \cdot A_{LM}(kr) + i\, \varphi^M_L(kr)\right] \psi_i \times \left\{ \int d\tau' \Phi_f^* \left[\alpha' \cdot A^*_{LM}(kr') - i\, \varphi^{M*}_L(kr')\right] \Phi_i \right\} \qquad (B.4)$$

where it is to be remembered that $\varphi_L^M = 0$ for electric and magnetic radiation. Carrying out the integration over ω, (B.4) becomes

$$U_{fo}' = \left(2\pi^2 e e' \frac{i}{k}\right) \left\{\int d\tau\, \Psi_f^* \left[\alpha \cdot B_{LM}(\omega r) + i\, \Psi_L^M(\omega r)\right] \Psi_i\right\} \times \left\{\int d\tau' \Phi_f^* \left[\alpha' \cdot A_{LM}^*(\omega r') - i\, \varphi_L^{M*}(\omega r')\right] \Phi_i\right\}$$

returning to (B.3) we note that from Appendix A,

$$\sum_{LM} \Psi_L^M(\omega r)\, \varphi_L^M(\omega r') = \left(\frac{\omega}{2\pi^2 i}\right) \frac{e^{i\omega x}}{x}$$

and

$$\sum_{LMi} \alpha \cdot B_{LM}^{(i)}(\omega r)\, \alpha' \cdot A_{LM}^{(i)*}(\omega r') = \sum \alpha \cdot B_{LM}^{(i)}(\omega r)\, A_{LM}^{(i)*}(\omega r') \cdot \alpha'$$

$$= \alpha \cdot \left(\frac{\omega}{2\pi^2 i}\right)\left(\frac{e^{i\omega x}}{x}\right) I \cdot \alpha' = \left(\frac{\omega}{2\pi^2 i}\right)\left(\frac{e^{i\omega x}}{x}\right)(\alpha \cdot \alpha')$$

Substitution of these results into (B.3) gives

$$U_{fo} = -e e' \int d\tau \int d\tau'\, \Psi_f^* \Phi^* (1 - \alpha \cdot \alpha') \left(\frac{e^{i\omega x}}{x}\right) \Psi_i \Phi_i$$

The same result is obtained for U_{fo} when r is less than r'.

2. Evaluation of $\int d\omega \left[\frac{H_{o\omega} H_{\omega o}}{\omega - k - i\eta} + \frac{H'_{o\omega} H'_{\omega o}}{\omega + \omega_o - i\eta}\right]$

following the same procedure as above, the integral reduces to

$$\int_{-\infty}^{\infty} d\omega \frac{|H_{o\omega}|^2}{\omega - k - i\eta} = \int_{-\infty}^{\infty} d\omega \frac{(\omega - k)|H_{o\omega}|^2}{(\omega - k)^2 + \eta^2} + i \int_{-\infty}^{\infty} d\omega \frac{\eta |H_{o\omega}|^2}{(\omega - k)^2 + \eta^2}$$

The first integral on the right represents the principal value part of the original integral and is usually neglected. In the second integral, $|H_{o\omega}|^2$ is a slowly varying function of ω. For small η, the denominator has a sharp minimum for $\omega = k$, so that the integrand has a sharp maximum. We may therefore take $|H_{o\omega}|^2$ outside the integral sign to replace it by its value at $\omega = k$, $|H_{ok}|^2$. Hence,

$$\int_{-\infty}^{\infty} d\omega \frac{|H_{o\omega}|^2}{\omega - k - i\eta} = i |H_{ok}|^2 \int_{-\infty}^{\infty} d\omega \frac{\eta}{(\omega - k)^2 + \eta^2} = i\pi |H_{ok}|^2 = i\gamma_1$$

where

$$|H_{ok}|^2 = \left(\frac{2\pi e'^2}{\omega}\right) \left| \int d\tau' \Phi_f^* \left[\alpha' \cdot A_{LM}^{(i)*}(\omega r') - i\, \varphi_L^{M*}(\omega r')\right] \Phi_i \right|^2$$

3. Evaluation of $\int dE \left[\frac{H_{\omega E}}{(E - k - i\eta)}\right]$, $\int dE \left[\frac{H'_{\omega E}}{(E - k - i\eta)}\right]$

In the manner as above we have,

$$\int dE \left[\frac{H_{\omega E}}{(E - k - i\eta)}\right] = i\pi H_{\omega k} \qquad \int dE \left[\frac{H'_{\omega E}}{(E - k - i\eta)}\right] = i\pi H'_{\omega k}$$

4. Evaluation of $\int d\omega \left[\frac{H_{o\omega} H_{\omega k}}{\omega - k - i\eta} + \frac{H'_{o\omega} H_{\omega k}}{\omega + \omega_o - i\eta} \right]$

Comparison of this integral with that denoted by U_{fo} and using Appendix A, we have that this integral is $U_{of} = U^*_{fo}$.

VITA

Buford Ray Anderson

Candidate for the Degree of

Master of Science

Thesis: DETERMINATION OF INTERNAL CONVERSION COEFFICIENTS BY THE SCINTILLATION METHOD

Major Field: Physics

Biographical:

Personal Data: Born in Berkeley, Kentucky, March 30, 1935, the son of Carl and Oma Anderson.

Education: Attended grade school in Berkeley, Kentucky and high school in Arlington, Kentucky; received a Bachelor of Science degree from Murray State College, Murray, Kentucky, in June, 1960; completed requirements for the Master of Science degree in November, 1962.

Experience: Entered the United States Army in 1954; was schooled in radio repair; received behind enemy lines combat training; spent a period of sixteen months overseas.

Organizations: Member of Sigma Pi Sigma and Pi Kappa Alpha.